IEEE Access
Multidisciplinary | Rapid Review | Open Access Journal

Received February 26, 2020, accepted March 15, 2020, date of publication March 18, 2020, date of current version March 27, 2020.

Digital Object Identifier 10.1109/ACCESS.2020.2981697

Robust Energy Management and Economic Analysis of Microgrids Considering Different Battery Characteristics

MOSTAFA H. MOSTAFA[1], SHADY H. E. ABDEL ALEEM[2], (Member, IEEE), SAMIA G. ALI[3], ALMOATAZ Y. ABDELAZIZ[4], (Senior Member, IEEE), PAULO F. RIBEIRO[5], (Fellow, IEEE), AND ZIAD M. ALI[6,7]

[1]Electrical Power and Machines Department, Faculty of Engineering, Ain Shams University, Cairo 11566, Egypt
[2]Mathematical, Physical and Engineering Sciences, 15th of May Higher Institute of Engineering, Cairo 11721, Egypt
[3]Electrical Power and Machines Department, Faculty of Engineering, Kafrelsheikh University, Kafrelsheikh 33511, Egypt
[4]Faculty of Engineering and Technology, Future University in Egypt, Cairo 11835, Egypt
[5]Advanced Power Technologies and Innovations in Systems and Smart Grids Group, Federal University of Itajuba, Itajuba 37500-903, Brazil
[6]Electrical Engineering Department, College of Engineering at Wadi Addawaser, Prince Sattam Bin Abdulaziz University, Wadi Addawaser 11991, Saudi Arabia
[7]Electrical Engineering Department, Aswan Faculty of Engineering, Aswan University, Aswan 81542, Egypt

Corresponding author: Shady H. E. Abdel Aleem (engyshady@ieee.org)

ABSTRACT This paper presents the economic analysis and optimal energy management of a grid-connected MG that comprises renewable energy resources and different battery storage technologies with different characteristics such as initial charge, depth of discharge, and the number of charging/discharging cycles to minimize the total operating cost of the system by maximizing the benefits of BSS, minimizing the investment and replacement cost of BSS, and minimizing the operation and maintenance cost of DGs. Several constraints are considered, such as the output power limits of the distributed generators, the limits of power imported from or exported to the grid, load balance, and other sets of battery storage constraints. The general algebraic modeling system (GAMS) is used to solve the deterministic optimization problem. Second, stochastic optimization is used to solve the deterministic problem with market price uncertainty. Third, robust optimization using the information gap decision theory is presented to model the electric load uncertainty. The validity and effectiveness of the proposed solution are explained by comparing the results obtained by GAMS to the results obtained by other optimization techniques presented in the literature.

INDEX TERMS Depth of discharge, distributed generation, energy management, energy storage, GAMS, microgrids, optimization.

ABBREVIATION

MG	Microgrid
GAMS	General algebraic modeling system
EM	Energy management
BSS	Battery storage system
MINLP	Mixed-integer nonlinear programming
MILP	Mixed-integer linear programming
DG	Distributed generation
IGDT	Information gap decision theory
SOS	Symbiotic organism search algorithm
CS	Cuckoo search algorithm
RES	Renewable energy sources
DOD	Depth of discharge
PV	Photovoltaic
WT	Wind turbine
FC	Fuel cell
MT	Micro-turbine
MGCC	Microgrid central controller
FS	Firefly search algorithm
KHS	Krill herd search algorithm

The associate editor coordinating the review of this manuscript and approving it for publication was Huaqing Li.

NOMENCLATURE

P_t^{PV}	Output power of the PV array
P_{rated}^{PV}	Rated power of the PV array
N^{PV}	Number of PV units
G	Global irradiation under standard test conditions in watts per square meter

G_0	Standard solar irradiation under standard test conditions in watts per square meter
T_A	Ambient temperature
T_C	Temperature coefficient of the maximum power of PV
η^{inv}	Efficiency of the inverter of the PV modules
η^{rel}	Relative efficiency of the PV modules
P_t^{WT}	Output power of the WTs
P_{rated}^{WT}	Rated power of the WTs
v_t^{WT}	Time step wind speed
v_{rated}^{WT}	Rated speed of the WT
v_{cut-in}^{WT}	Cut-in speed of the WTs
$v_{cut-out}^{WT}$	Cut-out speed of the WTs
$C_C^{battery}$	Capital cost of a BSS
C_{OM}	Operation and maintenance cost of the DGs
i_{t-MT}	Binary variable that decides the states of the MT
i_{t-FC}	Binary variable that decides the states of the FC
P_{M-t}	Output power of MT at time t
P_{FC-t}	Output power of FC at time t
P_{PV-t}	Output power of PV at time t
P_{WT-t}	Output power of WT at time t
b_{bat-FC}	Fixed operation and maintenance cost of the battery
P_{FC}	Output power of FC
η_{FC}	Efficiency of FC
c_{FC}	Fuel (natural gas) price to supply the FC in \$/kWh
c_{MT}	Fuel price to supply the MT in \$/kWh
P_{bat}	Rated power of the battery
E_{bat}	Rated capacity of the battery
b_{bat-P}	Power (\$/kW) rating cost of the battery
b_{bat-E}	Capacity (\$/kWh) rating cost of the battery
b_{grid-t}	Market energy price in (\$/kWh)
TIC_{BSS}	Total cost per day of the BSS through the lifetime of the project.
C_{grid-t}	Operation cost of the grid at time t
C_{DG-t}	Fuel cost of DGs at time t
P_{g-t}	Imported or exported power at time$t$
S_{MT-t}^{up}	Start-up cost of MT at time t
S_{FC-t}^{up}	Start-up cost of FC at time t
S_{MT-t}^{down}	Shut-down cost of MT at time t
S_{FC-t}^{down}	Shut-down cost of FC at time t
n_R	Number of replacements of BSSs
i	Working day
$m_{pcb}(t, i)$	Indicator of cycles performed as a function of t and i
P_{bat-t}^{ch}	Charged power of BSS
P_{bat-t}^{dis}	Discharged power of BSS
SOC_t	State of charge of BSS at time t

I. INTRODUCTION

Recently, much attention has been paid to means of developing centralized, producer-controlled traditional power grids to be smarter self-managing, and reliable grids that can produce, transmit, and use energy effectively, along with strengthened plans for environmental protection and pollution control. Also, the creation of economic incentives and increased usage of consumer-interactive renewable energy sources (RESs) remain the leading solutions to transit away from traditional high-carbon energy sources [1]–[4]. In this regard, a microgrid (MG) is projected as a localized consumer-interactive distribution network construction within the smart grid community, to achieve a low-carbon society with reduced greenhouse gas emissions, while taking into account the local-generation properties, variability in the generation inputs and economic aspects [5]–[7].

MGs comprise different types of distributed generation (DG) units, energy storage systems, and electrical loads, and can operate either with the grid (grid-connected mode) or without the grid (islanded mode) [8], [9] to create an efficient and more economical system with enhanced power quality and reliability performance levels, increased energy efficiency, and reduced environmental pollution [10], [11]. From the perspective of economic aspects, MG operators have to determine the optimal energy management (EM) that can accomplish the lowest operating, maintenance and capital costs over the lifetime of a project [12], while maintaining reliability, efficiency, and power quality considerations of production and consumption of electricity.

Energy storage is the key enabler for reliable MGs to become more resistant to disruptions, taking into account the increased generation of renewable electricity and reduced operation costs [13], [14].

There are different energy storage types that can be integrated into MGs to enhance their performance and management. Among these types, battery storage is an attractive option to use in MGs due to its technological maturity, reliability, and capability to provide appropriate power and energy densities [15], [16]. However, different battery characteristics obtained from the datasheets of the battery manufacturers, such as the depth of discharge (DOD) and numbers of charging/discharging cycles, determine the lifetime of battery storage systems (BSSs) [17], [18]. These characteristics vary from one battery to another; therefore, battery storage characteristics should be taken into consideration in the planning and operation of MGs because they have a significant influence on the stored energy that can be released during high demand periods or when renewables are unavailable, in addition to their impacts on the accuracy of the economic results of EM [18].

In recent literature, many works investigated different solutions to optimize the EM of MGs using constrained mathematical-based or heuristic-based optimization methods. For instance, Wang *et al.* [19] proposed a two-stage approach for determining the optimal EM of an MG with high penetration of RESs, while considering the intermittency

of the renewables, demand and day-ahead prices. The first stage aimed to minimize the operation cost of the MG, while the second one aimed to minimize real-time and day-ahead market costs imbalance. Nayak *et al.* [20] introduced an optimization approach to minimize the operation cost of an MG with fixed and variable loads while considering different types of BSS. Three management strategies were investigated in this approach. In the first strategy, the main grid and RESs were used to supply the load with no BSS connected. In the second one, the RESs with a BSS connected were used to supply the electricity load in isolated MG mode. In the third strategy, the main grid and RESs with the BSS connected were used to supply the load in a grid-connected mode. Hossain *et al.* [21], [22] presented a real-time EM optimization strategy of an MG to minimize its operation cost while considering the degradation cost of the battery. The mathematical modeling of the MG components such as photovoltaic (PV) units, wind turbines (WT), BSS, converter, and the main grid, was presented. Abedini *et al.* [23] developed an optimization method called guaranteed convergence particle swarm optimization with Gaussian mutation (GPSO-GM) to achieve the optimal EM of hybrid energy isolated MG by minimizing the capital, operation, and maintenance costs. The proposed algorithm is applied to a 69-bus and 94-bus MG to evaluate the performance of the proposed method. Iqbal *et al.* [24] proposed a mixed integer linear program (MILP) model using JuMP-Julia and Gurobi solvers for the EM of MGs considering grid-connected, grid-disconnected, and stand-alone strategies. Ruiz-Cortés *et al.* [25] developed a genetic algorithm-based approach to determine the optimal charge/discharge daily scheduling of batteries in grid-connected MG taking into account energy exchange loss minimization. Fathy and Abdelaziz [26] presented both single and multi-objective design algorithms to manage the operation of an MG. The single objective function aimed to minimize the total operating cost and emissions from the MG individually using krill herd (KHS) optimization. The multi-objective function aimed to minimize the total operating cost and emissions of the MG simultaneously using the ant lion optimizer. Sedighizadeh *et al.* [27] presented a stochastic multi-objective-based model for optimal economic–environmental energy and reserve scheduling of a grid-connected MG, considering traditional energy resources, RESs, and BSS. The Weibull, beta, and normal probability distribution functions were utilized to model uncertainties of the wind speed, solar radiation, and demand, respectively. Moradi and Eskandari [28] proposed a hybrid optimization approach to obtain the optimal capacity of DGs in order to determine the appropriate operational planning for the MG in the four seasons, considering uncertainty in electricity price forecasting using fuzzy mathematical programming. Fan *et al.* [29] and Narayan and Ponnambalam [30] presented multi-objective stochastic models based on Monte Carlo simulation to achieve optimal EM of grid-connected MGs under uncertainty. Tavakkoli *et al.* [31] presented the optimal EM of a grid-connected MG, integrating uncertainty and risk to minimize the risk and operational cost. The autoregressive integrated moving average model was applied to obtain the predicted value of electrical loads and PV units. Rui *et al.* [32] developed a mixed integer programming model and game model for optimal energy scheduling of multiple MGs. Mazzola *et al.* [33] proposed a framework to determine the optimal energy scheduling of isolated rural MGs considering forecast-based dispatch in the MGs operation using a normalized root-mean-square error approach. Mellouk *et al.* [34] formulated an optimization technique based on a genetic algorithm–particle swarm optimization algorithm to determine the optimal energy management of a grid-connected MG in Laayoune region. Ramli *et al.* [35] formulated a multi-objective self-adaptive differential evolution algorithm to design and manage the energy of a grid-connected MG.

Also, many research works used electric vehicles (EVs) as a favorable strategy to meet the increasing environmental concerns and energy storage in MGs. For instance, Esmaili *et al.* [36] presented an approach to minimize the operation cost and energy loss of a grid-connected MG, considering the range anxiety of EVs in energy management with different types of controllable loads to enhance the benefits. Igualada [37] formulated a MILP model to manage a residential MG, including a charging spot with a vehicle-to-grid system and renewable energy sources. The intermittent nature of RESs, energy consumption, market price, range anxiety, departure, and arrival times of EVs and their state of charge, were taken into account to minimize the operation cost of the MG. Three cases were considered to quantify the impact of range anxiety on the total cost of the MG. Yan *et al.* [38] proposed a stochastic optimization approach for the application of real-time EM of a grid-connected MG with battery swapping and renewables to minimize the operation cost. Alharbi and Bhattacharya [39] formulated a mathematical approach to manage the energy of an islanded MG from different perspectives, taking into account the demand response to provide flexibility in the MG operation, charging of EVs, and operation of BSSs. Mortaz and Valenzuela [40] presented a two-stage mathematical model to optimally schedule the energy of a grid-connected MG considering the uncertainty of the EVs' parking facility and the electric demands, EVs' parking time, battery degradation, and arrival and departure times. Lu *et al.* [41] proposed a multi-objective optimization model for the optimal dispatch of grid-connected MG with EVs to minimize the operation cost and environmental pollution of the MG. Coelho *et al.* [42] presented the design of a multi-objective MILP power dispatching model using plug-in EVs located at smart parks as storage units, considering the generation of different scenarios from probabilistic forecasting to scheduling the energy storage planning scenarios. Esmaeili *et al.* [43] proposed a bi-level scheduling framework of MG, including battery swapping stations as two independent stakeholders with both historical data-based and human-related uncertainties. An alternative direction method of a multipliers-based algorithm is utilized to solve the proposed optimization problem in a fully decentralized fashion.

Compared to the existing studies in this area, there are main differences between this work and the others. First, this study presents the economic analysis and optimal EM of a grid-connected MG comprising different battery storage technologies with different characteristics, such as initial charge, DOD, the number of charging/discharging cycles, or cost factors of BSSs, initially to select the most suitable BSS technology to integrate into the MG and then to minimize the total operating cost of the system by maximizing the benefits of BSS, minimizing the investment and replacement cost of BSS, and minimizing the operation and maintenance cost of DGs. It should be noted that most of the existing studies have not examined the impacts of the different battery characteristics, although these have significant influences on the planning and operation of MGs and affect the accuracy of the EM of these MGs. Second, in the proposed approach, stochastic optimization is used to solve the deterministic problem with market price uncertainty. The stochastic optimization utilizes several scenarios with corresponding probabilities to generalize a deterministic solution for the deterministic problem, varying some of the parameters in order to give a clearer picture of the impact of their variation on the solution. Third, robust optimization is employed to model the electric load uncertainty using information gap decision theory (IGDT). The IGDT is intended to obtain the optimal decisions to maximize the robustness of the objective function against the uncertainty parameter. Finally, a comparative analysis of the deterministic, stochastic and robust optimization methods is presented and discussed.

Hence, the main contribution of this study can be summarized as follows:

- A mathematical model to find the optimal EM of an MG is presented to minimize the total operation cost considering several economic factors. Due to the variety of characteristics of BSSs, four different BSS technologies are considered in the proposed model. Their technical and cost factors are taken into consideration to examine their suitability to be utilized in the examined grid-connected MG. Also, the impact of the DOD and the number of charging/discharging cycles of each BSS on the lifetime of the MG are investigated. Different initial charges and DODs of each BS type are also examined to achieve the optimal EM of the MG.
- A stochastic optimization approach is presented to solve the deterministic problem with market price uncertainty.
- A robust optimization using the IGDT method is applied to the hourly economic operation of the MG to model the electric load uncertainty.
- Presenting a model for risk-constrained over a day's scheduling period to minimize the cost under uncertain load.
- Proposing a model that optimizes the robustness of decision-making strategy.
- The validity and effectiveness of the proposed solution are confirmed by comparing the obtained results with the results obtained by other optimization methods.

The rest of the paper is organized as follows: Section II describes the MG configuration. Section III provides the mathematical formulation of the problem. Also, GAMS and its implementation to solve the problem are presented. In Section IV, we present the simulation results and discuss them. Finally, Section V presents a brief summary of the work done, conclusions drawn from the study, and future works.

II. SYSTEM CONFIGURATION

In what follows, the MG used to investigate the influence of the characteristics of the BSS on the total operation cost of the MG is presented. The typical MG considered comprises several DG systems such as a micro-turbine (MT), fuel cell (FC), photovoltaic (PV), wind turbine (WT) and BSSs, in addition to an MG central controller (MGCC) and loads as shown in Fig. 1 [44], [45]. The MG connects to the distribution system (main grid) via a point of common coupling (PCC).

A. PHOTOVOLTAIC (PV) UNITS

The output power of PV under the operating conditions depends on the solar radiation and temperature of the atmosphere, as given by (1) [46].

$$P_t^{PV} = N^{PV} P_{rated}^{PV} \left(\frac{G}{G_0}\right) (1 - T_C\,(T_A - 25))\,\eta^{inv}\eta^{rel} \tag{1}$$

where P_t^{PV} and P_{rated}^{PV} are the output and rated powers of the PV array, respectively, N^{PV} is the number of PV units, G and G_0 are the global irradiation and standard solar irradiation under standard test conditions in watts per square meter, respectively. T_A is the ambient temperature and T_C is the temperature coefficient of the maximum power of PV. η^{inv} and η^{rel} represent the efficiency of the inverter and the relative efficiency of the PV modules, respectively [47].

B. WIND TURBINE (WT) SYSTEM

The output power of WTs depends on the wind speed in a specific location and the power curve (given by the manufacturers of the WTs), which is expressed as a function divided into four parts as represented in (2). Also, the hourly wind speed is estimated using the Weibull distribution function from data in previous publications [46].

$$P_t^{WT} = \begin{cases} 0 & v_t^{WT} < v_{cut-in}^{WT} \\ P_{rated}^{WT}\left(\frac{(v_t^{WT})^3 - (v_{cutin}^{WT})^3}{(v_{rated}^{WT})^3 - (v_{cutin}^{WT})^3}\right) & v_{cutin}^{WT} \le v_t^{WT} < v_{rated}^{WT} \\ P_{rated}^{WT} & v_{rated}^{WT} \le v_t^{WT} < v_{cutout}^{WT} \\ 0 & v_t^{WT} \ge v_{cutout}^{WT} \end{cases} \tag{2}$$

where P_t^{WT} and P_{rated}^{WT} are the output power and rated power of the WTs, respectively, v_t^{WT} and v_{rated}^{WT} represent the time step wind speed and rated speed of the WT, respectively, and v_{cut-in}^{WT} and $v_{cut-out}^{WT}$ are the cut-in and cut-out speeds of the WTs.

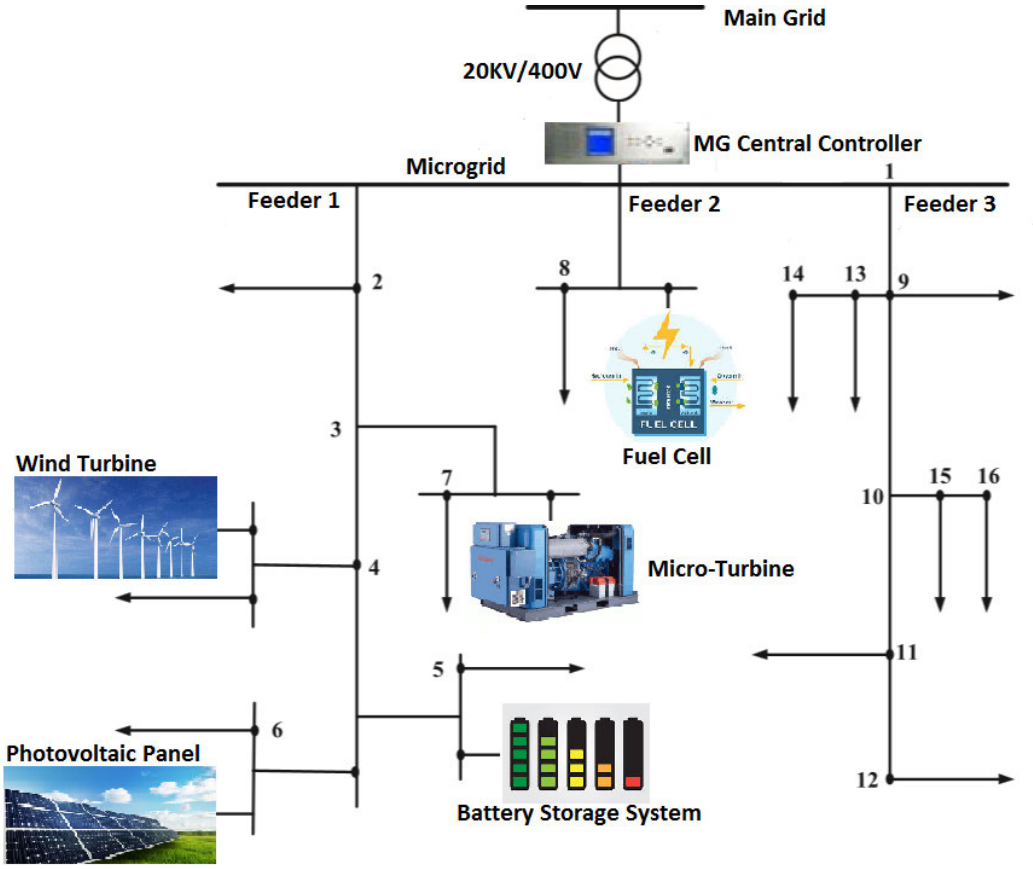

FIGURE 1. The MG under study.

C. FUEL CELL (FC)

FCs do not need conventional fuels; thus, they are considered clean energy sources because they eliminate the pollution caused by burning conventional fuels [48]. Also, they are simple to maintain and have a higher efficiency than diesel engines. In addition, the use of FCs, at the point of use, helps support the stability of decentralized MGs. FCs differ from batteries in their longer operating times and because they need a continuous source of fuel and oxygen to withstand the chemical reaction. The FC cost (C_{FC}) depends on the active output power (P_{FC}) and efficiency (η_{FC}) as given in (3) [49].

$$C_{FC} = C_{FC}\left(\frac{P_{FC}}{\eta_{FC}}\right) \tag{3}$$

where C_{FC} is the fuel (natural gas) price to supply the FC in \$/kWh. η_{FC} is the ratio of the actual operating voltage [48].

D. MICRO-TURBINE (MT)

MTs have many benefits compared to piston engines in terms of low maintenance costs, low emissions, small size, good reliability, and fuel flexibility. The MT cost (C_{MT}) depends on the active output power (P_{MT}) in kilowatts and the efficiency (η_{MT}) as given in (4) [50].

$$C_{MT} = C_{MT}\left(\frac{P_{MT}}{\eta_{MT}}\right) \tag{4}$$

where C_{MT} is the fuel price to supply the MT in \$/kWh.

E. BATTERY STORAGE SYSTEMS (BSSs)

There are various battery storage types, such as lead-acid, lithium-ion, sodium sulfur, nickel cadmium, etc. [15]. Each of them has its own technical features that influence the power quality measures, peak load reduction, grid stability, hosting more RES, and the EM of the system [46], [52]. The capital cost of a BSS $\left(C_C^{battery}\right)$ depends on its size in terms of power (\$/kW) and energy capacity (\$/kWh) as in (5).

$$C_C^{battery} = (b_{bat-P} \times P_{bat}) + (b_{bat-E} \times E_{bat}) \tag{5}$$

where P_{bat} and E_{bat} are the rated power and capacity of the battery, respectively, and b_{bat-P} and b_{bat-E} are the power (\$/kW) and capacity (\$/kWh) rating cost of the battery.

It should be noted that the BSS influences the MG planning and operation costs significantly, where an increase in the battery size increases the investment cost in a linear manner, whilst it reduces the operation cost in a nonlinear manner [15].

In this respect, the most developed battery type is the lead-acid battery (LA). The capital cost of LA batteries is inexpensive compared to other types of BSS; however, they may not be a suitable choice for minimizing the operational costs of MGs due to their short lifetime. The efficiency of LA batteries is around 70% [5]. Nickel-cadmium (NiCd) batteries have many advantages compared to LA batteries, such as their longer lifetime, lower internal impedance, higher energy

density, and better low-temperature performance; however, both cadmium and nickel are heavy metals that have adverse effects on human health. The efficiency of NiCd batteries is around 85%. Furthermore, sodium-sulfur (NaS) batteries are the most promising battery technologies because they are relatively inexpensive, have a high energy storage capacity, efficiency, and low weight. The efficiency of NaS batteries is about 90%. Also, lithium-ion (Li-ion) batteries have many advantages, such as their high specific energy, high efficiency, high energy density, high open-circuit cell voltage, fast charge and discharge response, and low weight. However, the capital cost of Li-ion batteries is very high compared to the other types. The efficiency of Li-ion batteries is about 98% [15], [19], [52]. Additionally, there are other criteria that affect the operation of BSSs, such as degradation, depth of discharge and number of cycles.

F. OPERATION COST OF THE MAIN GRID

The operating cost of the main grid (C_{grid}) depends on the electrical power (P_g) and market energy price (b_{grid}) in (\$/kW) as given in (6).

$$C_{grid} = b_{grid} \times P_g \tag{6}$$

III. PROBLEM FORMULATION

This section presents the formulation of the optimization problem to find the optimal EM of an MG to minimize the total operation cost considering several economic factors. The objective function, constraints, and search algorithm using GAMS are presented. Further, a stochastic optimization method is introduced to model the uncertainty of the energy market price depending on its historical data and probabilistic density function. Then, robust optimization using information gap decision theory is presented to model the electric load uncertainty.

A. PROBLEM STATEMENT

Energy management of MGs that comprise different types of DG units, BSS, and electrical loads is essential to minimize the operation cost of such localized grids and allow the use of RES in an efficient manner.

BS is the key enabler for reliable MGs to reduce their operation cost by storing energy during the off-peak time and then discharging this energy during peak times. Unfortunately, the investment cost of the BSS is still high. Therefore, the charge/discharge of BSS should be carefully scheduled to achieve the maximum benefits from BSSs. For that reason, this study aims to find the optimal EM of grid-connected MGs to minimize the total operating cost of the system.

Various constraints are taken into consideration such as the output power limits of DGs, limits of the power imported from or exported to the grid, load balance and another set of BSS constraints such as power and energy capacity, limits of the state of charge taking into account the BSS type, efficiency, initial charge, DOD value, and life cycle.

The concept procedure proposed to manage the energy of the studied MG is illustrated in Fig. 2, in which the MGCC is responsible for realizing a satisfactory automated operation of the MG by utilizing real-time data of the DGs, main grid, energy market price, and controlling electrical loads to perform an active hourly generation schedule in an economical manner. The proposed approach can be used by the MGCC to optimize the MG operation, according to forecasted data of WT, PV, and loads for a 24-hour period, limits the power of each DG, technical and economic factors of BSS, and the 24-hour market price of the main grid and sends signals to the local controller of the DGs units, BSS, and loads centers to control the output power of each DG, load, charging/discharge of BSS, and power imported from or exported to the grid. Renewable energy sources (WT and PV) are given priority in the operation of MG. The objective of priority-based energy management is to minimize the operational cost of the MG and increase the penetration level of renewable energy sources. The objective of priority-based energy management is to minimize the operational cost of the MG and allow the use of RES in an efficient manner.

The mathematical formulation of the optimization problem is given as follows:

B. OBJECTIVE FUNCTION

The objective function *(OF)* is to minimize the total operating cost of the MG, $f(x)$. Mathematically, $f(x)$ is divided into three parts as given in (7), in which the first part (C_t) expresses the operation cost of the main grid (\$/kWh), generation costs of DGs (\$/kWh), and start-up and shut-down costs of the MT and FC, the second part (C_{OM}) expresses the operation and maintenance cost of the DGs, and the third part (TIC_{BSS}) expresses the total cost per day of the BSS through the lifetime of the project.

$$OF = min f(x) = \sum_{t=1}^{T} (C_t + C_{OM} + TIC_{BSS}) \tag{7}$$

where t is the time step in hours (h) and T denotes the 24-hour horizon. C_t is expressed as follows:

$$C_t = C_{grid-t} + C_{DG-t} + \left(S^{up}_{MT-t} + S^{down}_{MT-t}\right) + \left(S^{up}_{FC-t} + S^{down}_{FC-t}\right) \tag{8}$$

where C_{grid-t} and C_{DG-t} are the operation cost of the main grid at time t (\$/kWh) and the fuel costs of DGs at time t (\$/kWh), respectively. C_{grid-t} is calculated as given in (9), where b_{grid-t} is the market energy price in (\$/kWh) and P_{g-t} is the imported or exported power at time t, in which a negative value shows power export to the grid and the positive one denotes power import from the grid.

$$C_{grid-t} = b_{grid-t} \times P_{g-t} \tag{9}$$

The generation cost of DGs at time t (C_{DG-t}) is given in (10).

$$C_{DG-t} = (b_{MT-t} \times P_{MT-t})\, i_{t-MT} + (b_{FC-t} \times P_{FC-t})\, i_{t-FC} + (b_{PV-t} \times P_{PV-t}) + (b_{WT-t} \times P_{WT-t}), \quad \forall t \in T \tag{10}$$

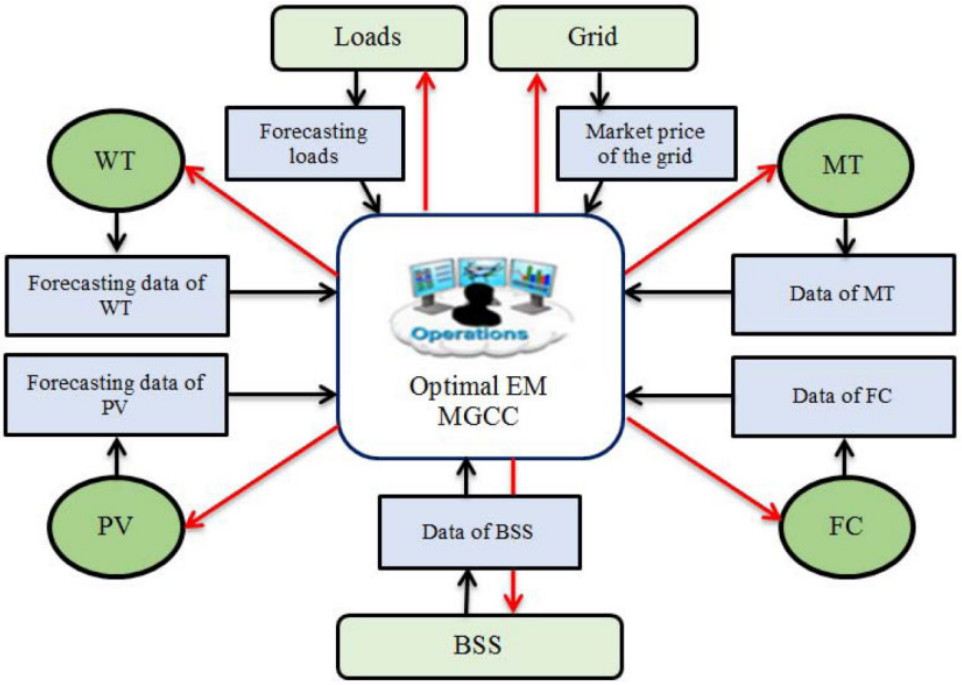

FIGURE 2. Concept procedure proposed to manage the energy of the MG under study.

i_{t-MT} and i_{t-FC} are binary variables that decide the states of the MT and FC, respectively, in which the binary variable i_{t-MT} or i_{t-FC} equals 1 when the MT or FC is on; otherwise, i_{t-MT} or i_{t-FC} equals 0 when the MT or FC is off. Also, b_{MT-t}, b_{FC-t}, b_{PV-t}, and b_{WT-t} are the bidding prices of the MT, FC, PV, and WT (\$/kWh) at time t, respectively. P_{M-t}, P_{FC-t}, P_{PV-t} and P_{WT-t} are the output powers of the MT, FC, PV, and WT at time t.

Moreover, the start-up and shut-down costs of the MT and FC are expressed by (11)–(14).

$$S^{up}_{MT-t} = b^{up}_{MT} \times max\left(0, \left(i_{t-MT} - i_{(t-1)-MT}\right)\right), \quad \forall t \tag{11}$$

$$S^{down}_{MT-t} = b^{down}_{MT} \times max\left(0, \left(i_{(t-1)-FC} - i_{t-FC}\right)\right), \quad \forall t \tag{12}$$

$$S^{up}_{FC-t} = b^{up}_{FC} \times max\left(0, \left(i_{t-FC} - i_{(t-1)-FC}\right)\right), \quad \forall t \tag{13}$$

$$S^{down}_{FC-t} = b^{down}_{FC} \times max\left(0, \left(i_{(t-1)-FC} - i_{t-FC}\right)\right), \quad \forall t \tag{14}$$

where S^{up}_{MT-t} and S^{up}_{FC-t} are the start-up costs of the MT and FC at time t, respectively. S^{down}_{MT-t} and S^{down}_{FC-t} are their shut-down costs at time t, respectively. Moreover, b^{up}_{MT} and b^{up}_{FC} are the start-up cost coefficients (\$) of the MT and FC, respectively, and b^{down}_{MT} and b^{down}_{FC} are their shut-down cost coefficients, respectively.

Then, the second part of $f(x)$ that represents the total operation and maintenance cost (C_{OM-t}) at time t is expressed as the summation of the tth operation and maintenance costs of the MT, FC, PV, and WT denoted by C^{MT}_{OM-t}, C^{FC}_{OM-t}, C^{PV}_{OM-t} and C^{WT}_{OM-t}, respectively, in (15).

$$C_{OM-t} = C^{MT}_{OM-t} + C^{FC}_{OM-t} + C^{PV}_{OM-t} + C^{WT}_{OM-t} \tag{15}$$

Finally, the third part of $f(x)$ that represents the total cost of the BSSs used per day (TIC_{BSS}) comprises capital $\left(C^{battery}_{C}\right)$ and operating and maintenance $\left(C^{battery}_{OM}\right)$ costs, in addition to costs related to the number of replacements of BSSs (n_R) along the project's lifetime (N). Both $C^{battery}_{C}$ and $C^{battery}_{OM}$ depend on the size of the BSS in terms of power (\$/kW) and energy capacity (\$/kWh) as represented in (5) and (16).

$$C^{battery}_{OM} = (b_{bat-FC} \times P_{bat}) + (b_{bat-VC} \times W_{bat}) \tag{16}$$

where b_{bat-FC} and b_{bat-VC} denote the fixed and variable operation and maintenance costs of the battery per year (\$/kWh/yr). W_{bat} is the annual discharge of the battery (kWh/yr).

To determine n_R; first, the total number of cycles performed through the battery ($PC_{battery}$) is determined using (17) and (18) to determine the battery lifetime. Thus:

$$m_{pcb}(t, i) = \left(x_{b(t)} - x_{b(t-1)}\right) x_{b(t)}, \quad \forall t \in T, \ \forall i \in d \tag{17}$$

$$PC_{battery} = \sum_{i=1}^{d} \sum_{t=1}^{T} m_{pcb}(t, i) \tag{18}$$

where $m_{pcb}(t, i)$ is an indicator of the cycles performed as a function of t and i, where i denotes the working day and d is the total number of working days, which is set in this work to 365. $x_{b(t)}$ is a binary variable that shows the operating status of the BSS at t and i, in which x_b is equal to 1 when the BSS is charging and 0 when the BSS is discharging.

Second, the life cycle of a battery depends on its DOD; therefore, the expected lifetime ($ELTB_{DOD}$) of a battery at a certain DOD depends on its life cycle at the same DOD (BLC_{DOD}) and the $PC_{battery}$ as expressed in (19).

$$ELTB_{DOD} = \frac{BLC_{DOD}}{PC_{battery}} \tag{19}$$

Hence, n_R can be expressed as follows:

$$n_R = \frac{N}{ELTB_{DOD}} \tag{20}$$

Accordingly, TIC_{BSS} is expressed as:

$$TIC_{BSS} = \frac{\left(C_C^{battery} + C_{OM}^{battery}\right) \times n_R}{N \times d} \tag{21}$$

C. CONSTRAINTS

The objective function is subject to the following constraints:

1) ENERGY STORAGE LIMITS

There are several ES limits that should be considered in the problem formulation. The first limit given by (22) expresses the charged power $\left(P_{bat-t}^{ch}\right)$ with respect to the maximum charging capacity limit of the BSS $\left(P_{bat-t}^{ch-max}\right)$. Similarly, the second limit, given by (23), is to ensure that the discharged energy $\left(P_{bat-t}^{dis}\right)$ is less than the maximum discharging capacity limit of the BSS $\left(P_{bat-t}^{dis-max}\right)$. The limits of the state of charge of BSS with respect to the minimum and maximum limits are represented by (24).

$$P_{bat-t}^{ch} \le P_{bat-t}^{ch-max}, \quad \forall t \le T \tag{22}$$

$$P_{bat-t}^{dis} \le P_{bat-t}^{dis-max}, \quad \forall t \le T \tag{23}$$

$$SOC_t^{min} \le SOC_t \le SOC_t^{max}, \quad \forall t \le T \tag{24}$$

Also, the amount of charged power with the efficiency (η_{bat}) of the battery considered should be equal to the amount of the discharged power as represented by (25).

$$\sum_{t=1}^{T} P_{bat-t}^{dis} = \sum_{t=1}^{T} P_{bat-t}^{ch} \times \eta_{bat} \tag{25}$$

The state of charge of the battery (SOC_t) is based on the previous state of charge of the battery (SOC_{t-1}) and the discharge and charge quantity at time t as given in (26). It should be noted that, in the first period ($t = 1$), the initial SOC (SOC_0) needs to be considered.

$$SOC_t = \begin{cases} SOC_0 + \eta_{bat} P_{bat-t}^{ch} \Delta t - \Delta t P_{bat-t}^{dis} & t = 1 \\ SOC_{t-1} + \eta_{bat} P_{bat-t}^{ch} \Delta t - \Delta t P_{bat-t}^{dis}, & \forall t \ge 2, t \in T \end{cases} \tag{26}$$

However, the state of charge at the last period should equal SOC_0 to maintain the state of charge constant, as expressed in (27). Furthermore, the battery aging constraint is represented by (28).

$$SOC_t = SOC_0, \quad t = T \tag{27}$$

$$BLC_{DOD} \ge \sum_{i=1}^{d} \sum_{t=1}^{T} m_{pcb}(t, i) \tag{28}$$

2) BALANCE OF LOADS

At time t, the total power generated from the MT, FC, PV, WT, the power imported from (or exported to) the grid, and power discharged from (or charged to) the battery should equal the total load (P_{L-t}) power as given in (29).

$$P_{MT-t} i_{t-MT} + P_{FC-t} i_{t-FC} + P_{PV-t} + P_{WT-t} + P_{g-t} + P_{bat-t}^{dis} = P_{L-t} + P_{bat-t}^{ch}, \quad \forall t \tag{29}$$

3) GRID'S ACTIVE POWER LIMIT

The power imported from or exported to the grid (P_{g-t}) should be within its limits at each time as in (30).

$$P_{g-t}^{min} \le P_{g-t} \le P_{g-t}^{max}, \quad \forall t \tag{30}$$

4) DG'S POWER LIMITS

The output power of the MT, FC, PV, and WT should be within their specified limits as given in (31)–(34).

$$P_{MT-t}^{min} \le P_{MT-t} \le P_{MT-t}^{max}, \quad \forall t \tag{31}$$

$$P_{FC-t}^{min} \le P_{FC-t} \le P_{FC-t}^{max}, \quad \forall t \tag{32}$$

$$P_{PV-t}^{min} \le P_{PV-t} \le P_{PV-t}^{max}, \quad \forall t \tag{33}$$

$$P_{WT-t}^{min} \le P_{WT-t} \le P_{WT-t}^{max}, \quad \forall t \tag{34}$$

D. STOCHASTIC OPTIMIZATION TO TAKE ACCOUNT OF MARKET PRICE UNCERTAINTY

Stochastic optimization is used to solve the deterministic problem with market price uncertainty. The stochastic optimization utilizes several scenarios with corresponding probabilities to generalize a deterministic solution for the deterministic problem with the variation of some parameters in order to give a clearer picture of the impact of their variation on the solution [53], in which the available data for market price refers to hourly electric price data, i.e., the dimension of patterns is $D = 24$. Each daily electric price curve is expressed with a vector with D = 24. The fuzzy c-means clustering (FCM) technique [54], [55] was employed for generating a pre-set number of clustered scenarios (W) out from the normally distributed 8760 scenarios. A high number of clusters is not recommended since it refers to increased complexity on the operation system [56], [57]. In this study, the FCM was used to group a certain number of data (N) into W clusters, where W is set to 5.

The data required to be clustered are gathered in a matrix A including a set of column vectors a_j where $j \in \{1, 2, \ldots .N\}$. FCM requires two essential parameters to group A: W and the component of fuzziness (q), where $q \in R$, and $q > 1$. A pre-set tolerance (ε) is assumed for terminating the optimization process. The algorithm of FCM clustering passes through five stages as follows:

Stage 1: A membership matrix ($R = \left[R_{ij}\right]_{W \times N}$) is initialized randomly where the sum of each column j in R must equal 1. A W random centroids are chosen first from the given data. These centroids are gathered in a vector $= [W_i]_{1 \times W}$.

Stage 2: Calculate the new centroids using (35):

$$W_i = \frac{\sum_{i=1}^{N} R_{ij}^q \cdot a_j}{\sum_{i=1}^{N} R_{ij}^q} \tag{35}$$

Stage 3: Calculate the elements of the membership matrix ($R = [R_{ij}]_{W\times N}$) for each element in A, where

$$R_{ij} = \frac{1}{\sum_{p=1}^{W}\left(\frac{\|a_j - W_i\|}{\|a_j - W_p\|}\right)^{\frac{2}{q-1}}} \tag{36}$$

Stage 4: Calculate $f_{FCM}^{(m)} = \sum_{j=1}^{N}\sum_{i=1}^{W} R_{ij}^{q}\|a_j - W_i\|$, where $f_{FCM}^{(m)}$ is the objective function value at iteration m.

Stage 5: If $\left\|f_{FCM}^{(m)} - f_{FCM}^{(m-1)}\right\| < \varepsilon, \forall m > 1$, stop the optimization procedure, otherwise repeat the optimization procedure starting from Stage 2.

The stochastic operation cost ($/kWh) of the grid at time t considers 5 market price scenarios (S) and their probabilities (λ_s), which are obtained by FCM, expressed in (37) to solve the objective function given in (8).

$$C_{grid-t} = \sum_{s=1}^{S} \lambda_s \times b_{grid-t,s} \times P_{g-t} \tag{37}$$

E. ROBUST OPTIMIZATION MODEL USING INFORMATION GAP DECISION THEORY

IGDT is an approach for decision-making problems related to uncertainty that does not comprise any measure function, neither probabilistic density nor fuzzy membership functions [58]. This approach specifies as to what extent the uncertain parameter can change while assuring the minimum income for the decision-maker. Robustness and opportuneness are two basic styles for IGDT. These two inconsistent concepts stem from uncertainties of diverse parameters [59]. The robustness evaluates the resiliency to failure and opportuneness search for the chance of a windfall. The robustness and opportuneness can be illustrated as shown in Fig. 3. In Fig. 3(a) the decision-maker decreases the minimum profit to handle a more substantial part of the uncertain space. But, in Fig. 3(b) the decision-maker is optimistic about the uncertainties of the system, and the more the uncertain variables deviate from the forecasted amount (in an advantageous way), the more profit is gained [60], [61].

The robust system model of uncertainty is specified by $C(z, P_u)$, which represents the input/output structure of the system, in which $C(z, P_u)$ is explained as the reward of the decision-maker for selected values of variable z when considering the uncertain parameter P_u. In this work, the impact of the load uncertainty on the deterministic solution is investigated as given by (38) and (39):

$$P_u \in U(\alpha, \widetilde{P}_u) \tag{38}$$

$$U\left(\alpha, \widetilde{P}_u\right) = \left|\frac{P_u - \widetilde{P}_u}{\widetilde{P}_u}\right| \le \alpha \tag{39}$$

where the uncertainty horizon of parameter P_u is specified by α, and the expected value of P_u and the set of all values of P_u whose deviation from $\widetilde{P}_u$ is greater than $\alpha\widetilde{P}_u$ is denoted by $\widetilde{P}_u$ and $U\left(\alpha, \widetilde{P}_u\right)$, respectively [59].

The IGDT model helps the MGCC to reach robust decisions against high operating costs with respect to uncertainty in the total loading. Accordingly, a robustness function is utilized to achieve this target, in which $\tilde{\alpha}(z, C_o)$ expresses the information-gap robustness function that is interpreted as the maximum value that α can take while satisfying the minimum required value of the decision-making problem specified by the critical cost (C_c). Thus:

$$\begin{aligned}\tilde{\alpha}(z, C_c) &= max_{\alpha}\{\alpha : min\ C_c\ is\ always\ satisfied\}\\ &= max_{\alpha}\left\{\alpha : min_{P_u\in U(\alpha,\widetilde{P}_u)}\ C(z, P_u) \ge C_c\right\}\end{aligned} \tag{40}$$

Then, the performance of the robustness function is modeled by (41).

$$\begin{aligned}\tilde{\alpha}(z, C_c) = max_{\alpha}\Big\{\alpha : max_{P_u\in U(\alpha,\widetilde{P}_u)} C(z, P_u) \le C_c\\ = C_o(1+6)\Big\}\end{aligned} \tag{41}$$

where C_o is the minimum cost expected for the deterministic case taking into account the base load profile. σ is a cost deviation factor employed to determine the maximum allowable cost [60]. Consequently, the objective function will be modified to maximize the uncertainty horizon expressed by α, while considering the total cost budget that can be determined based on σ values. However, it should be noted that, for any value of α, the operating cost of the MG would be less than the highest operating cost. The modified formulation of the problem is expressed by (42).

$$\tilde{\alpha}(z, C_c) = max\ \alpha \tag{42}$$

subject to (22) – (28), (30) – (34), and

$$\sum_{t=1}^{T}(C_t + C_{OM} + TIC_{BSS}) \le C_o(1+6) \tag{43}$$

$$\begin{aligned}P_{MT-t}i_{t-MT} + P_{FC-t}i_{t-FC} + P_{PV-t} + P_{WT-t} + P_{g-t} + P_{bat-t}\\ = (1+\alpha)\times\widetilde{P_{L-t}}\end{aligned} \tag{44}$$

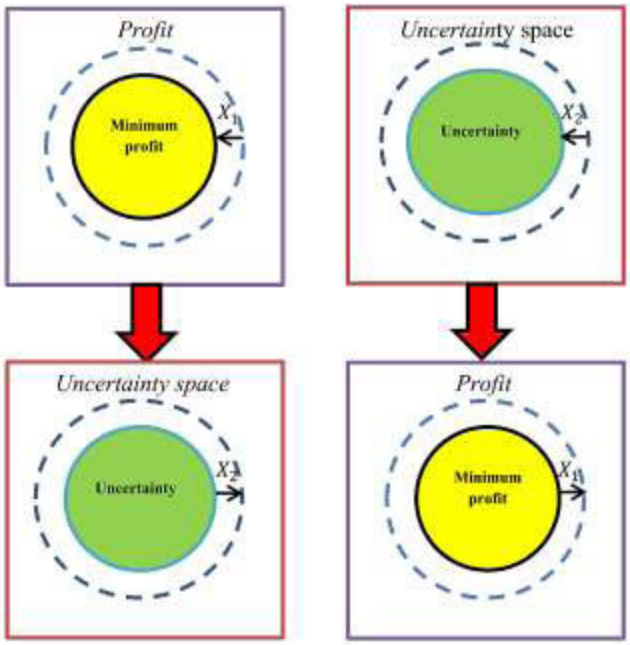

FIGURE 3. Concepts of (a) robustness strategy and (b) opportuneness concept.

Finally, after finding the maximum value of α by solving the optimization problem given by (42), the robust strategy will be determined on the basis of the value of C_c.

F. GENERAL ALGEBRAIC MODELING SOFTWARE (GAMS)

GAMS is a high-level optimization platform for solving linear, nonlinear, quadratic, and mixed-integer nonlinear optimization problems [62]. It is mainly used to solve complex problems using its different solvers including CONOPT, DICOPT, KNITRO, and CPLEX, to attain accurate results platforms [63], [64]. Also, it has the advantages of data integrity to ensure the proper functioning of a model. Several solvers for mathematical models have been hooked up to GAMS. The selection of an appropriate solver depends on the type of problems [65]. Fig. 4 shows the process of solving the studied problem using GAMS. After running the GAMS program to solve a complex problem, the solution report shows first the name of the model and the name of the objective function. Second, the type of the model is a linear, nonlinear, quadratic or mixed-integer nonlinear model and the direction of the optimization (maximization or minimization) is reported. Third, the name of that solver used for solving the model is reported. Fourth, the solution report shows the solver and model status, where each solver status code shows the error type and each model status code provides useful information regarding the global solution or local and so on. For example, the solver status is 1 (normal completion) means that the model is functioned without error. The model status is 1 (optimal) means a global solution is found [62]–[65].

IV. SIMULATION RESULTS AND DISCUSSION

A. DETERMINISTIC SOLUTION

In this section, the results obtained for the optimal EM of the considered MG in four cases are presented and discussed. For the MG shown in Fig. 1, Fig. 5 illustrates the hourly predicted output power of PV and WT on a typical day.

Table 1 provides the coefficients used, and the maximum and minimum power limits of the different DGs integrated into the MG. Moreover, Fig. 6 shows the hourly predicted total load and market energy price during a typical day [44], [45], [66].

Four battery types, namely, LA, NiCd, Li-ion, and NaS with different DOD values, are used. The cost and technical parameters of these batteries are presented in Table 2 [15].

The solver status has returned 1 in the solution report of GAMS/CPLEX, which indicates that the problem is solved without errors. Also, the model status was 1, which means that the solution to the problem is the global solution.

The impact of varying the DOD values of the BSSs and their expected life cycles is given in Table 3 based on the data sheets provided by the different battery manufacturers, in addition to the data available in the literature [15]. In the base case (case 0), the EM is executed with no BSS considered. In the first case (case 1), the EM is executed, including 4 BSSs, assuming they have zero initial charges. In the second case (case 2), the EM is executed using half-charged BSSs, and in the third case (case 3), fully charged BSSs are used. Also, in each case, multi-scenarios are considered to examine the impact of the different battery types and characteristics on the EM of the MG, while determining the optimal BSS technology, DOD value, initial charge, output power of each

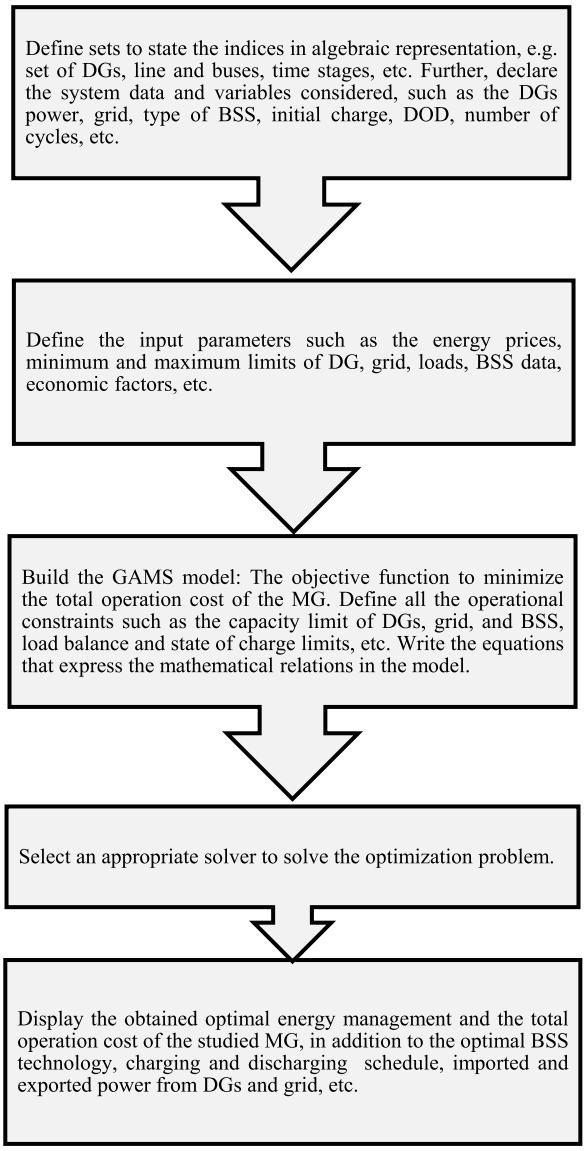

FIGURE 4. Process of solving the studied problem using GAMS.

TABLE 1. Data of DGs and main grid.

Unit	Minimum power (kW)	Maximum power (kW)	Bid ($/kWh)	Operation& maintenance cost ($/kWh)	Start-up/shut-down cost ($)
WT	--	15	1.72	0.24	0
PV	--	25	2.8	0.19	0
MT	6	30	1.32	0.59	0.96
FC	3	30	0.98	0.47	1.65
Grid	–40	40	Variable*	NA**	NA

*The bid is shown in Fig. 5
**NA: Not applicable

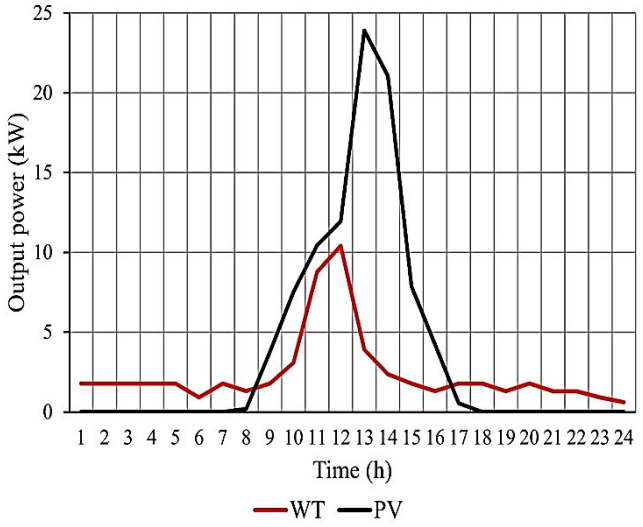

FIGURE 5. Hourly forecast output powers of WT and PV.

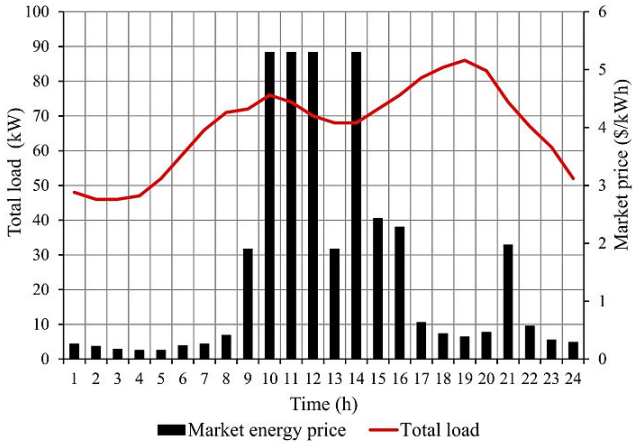

FIGURE 6. Hourly forecast values of the total load demand and market price during a typical day.

TABLE 2. Cost and technical parameters of BSSs.

Battery	Capital power cost ($/kW)	Capital energy cost ($/kWh)	Annual maintenance cost ($/kW)	Efficiency (%)
LA	200	200	50	70
NaS	350	300	80	95
Li-ion	900	600	--	98
NiCd	500	400	20	85

TABLE 3. Life cycles of the BSSs used with various DOD values.

DOD	Number of cycles			
	LA	NaS	Li-ion	NiCd
100	350	4000	3000	500
90	390	5000	3700	600
80	450	6000	4500	700
70	500	7000	5800	800
60	590	9000	6900	900
50	700	10000	8000	1200

DG, power from or to the grid, and the charging/discharging output of the BSS. The MILP is initially implemented in GAMS and solved using the CPLEX solver. Further, the validity and effectiveness of the solution are explained by comparing the results to the results obtained by other optimization methods: SOS, FS, CS, and KHS search algorithms. Next, we discuss the results obtained.

TABLE 4. The total operating cost of the MG with no BSS.

Solution method	Total operation cost of the MG per day ($)	Number of iterations
GAMS	1861.57	26
SOS	1902.38	1000
KHS	1961.09	1000
FS	1972.32	1000
CS	2032.49	1000

1) ENERGY MANAGEMENT WITH NO BSS INCLUDED: CASE 0

EM is executed with no BSS connected to the MG. Table 4 presents the results obtained by using the different optimization techniques GAMS, SOS, KHS, FS, and CS.

It is noted from the results presented in Table 5 that the GAMS solver provides the lowest total operating cost and converges in a few iterations (26 iterations) compared to the results obtained in 1000 iterations by the other optimization algorithms.

The optimal hourly output powers obtained by GAMS of the PV, WT, MT, FC, and utility during the day are shown in Fig. 7, which clarifies that the contribution of the renewable resources to supply the loads with no energy storage units is low compared with the contribution of the conventional non-renewable sources.

2) ENERGY MANAGEMENT USING ZERO CHARGED BSSS: CASE 1

In case 1, the EM is executed using four initially zero-charged BSS types. Recalling the life cycles of the BSSs presented in Table 3, and the total number of cycles performed through each battery ($PC_{battery}$); the expected lifetime ($ELTB_{DOD}$) of each battery, per year, is determined considering various DOD values, and the results obtained using GAMS are given in Table 5. TIC_{BSS} of the battery and the total operating cost of the MG are also presented in Table 6. The results show that the total operating cost of the MG depends considerably on the type of the battery and the DOD value.

We can see from Table 5 that the NaS battery has provided the best results compared to the results obtained using the other batteries. Fig. 8 shows the variation of the *SOC* of the NaS battery versus the DOD and time of day in case 1.

It can be noted from Tables 3 and 5 that the number of cycles of the batteries increases with the decrease of the permitted DOD value. Thus, $ELTB_{DOD}$ will increase and both n_R and TIC_{BSS} will decrease. This is also justified by the results given in Table 5 using the other battery types, as one can see that NiCd is not a suitable selection because of its high capital cost and short lifetime, meaning that it will have to be replaced many times along the project lifetime. Moreover, while the LA battery has a lower cost than the other batteries, its usage resulted in the lowest saving percentage because of its low efficiency and short lifetime. Although the

TABLE 5. Numerical results obtained in case 1.

Case 1		$PC_{battery}$	$ELTB_{DOD}$	n_R	TIC_{BSS} ($)	Total cost per day ($)	$Saving$ (%)
BSS	DOD (%)						
LA	100	730	0.479	32	154.9	1660.5	10.82
	90	730	0.534	28	136.1	1670.6	10.28
	80	730	0.616	25	121.9	1685.6	9.47
	70	730	0.685	22	107.8	1700.5	8.67
	60	730	0.808	19	93.64	1715.4	7.87
NaS	100	730	5.479	3	27.5	1458.8*	21.65*
	90	730	6.85	3	27.5	1487.3	20.12
	80	730	8.219	2	20.5	1514.3	18.67
	70	730	9.589	2	20.5	1548.2	16.85
	60	730	12.329	2	20.5	1582.2	15.02
Li-ion	100	1095	2.74	6	89.1	1512.9	18.75
	90	1095	3.379	5	74.3	1526.9	17.99
	80	1095	4.109	4	59.4	1546.5	16.94
	70	1095	5.297	3	44.6	1566.1	15.89
	60	1095	6.301	3	44.6	1600.4	14.05
NiCd	100	730	0.685	22	210.9	1667.3	10.45
	90	730	0.822	19	182.4	1665.7	10.54
	80	730	0.959	16	153.8	1669.5	10.33
	70	730	1.095	14	134.8	1682.8	9.62
	60	730	1.233	13	125.3	1705.7	8.39

* The values in bold represent the best results obtained.

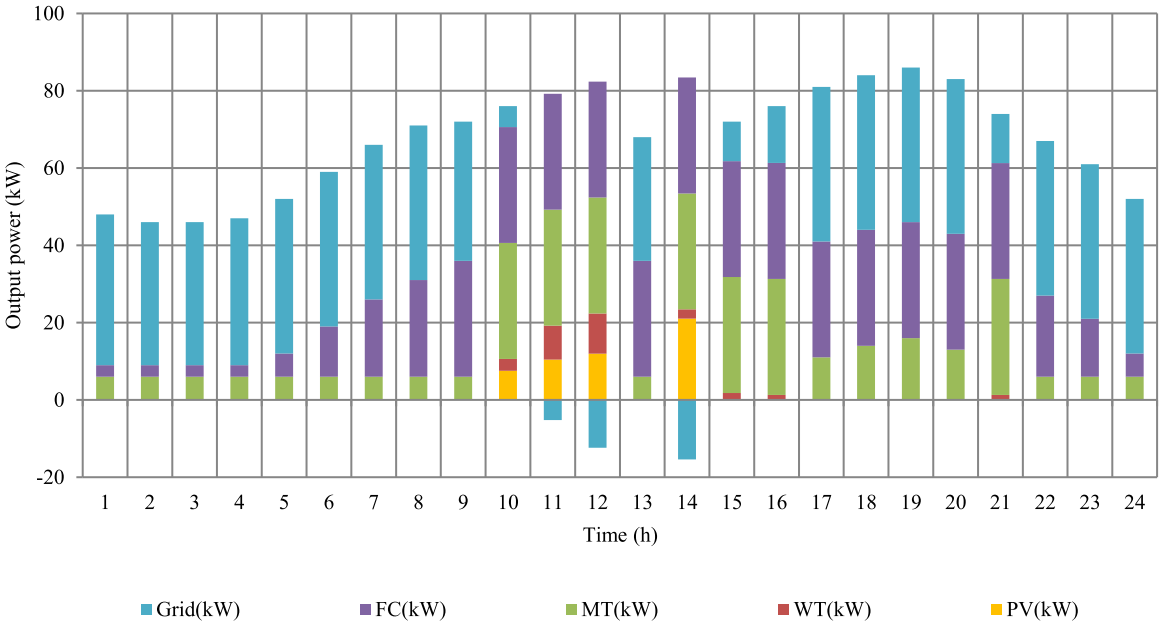

FIGURE 7. Optimal hourly output powers of PV, WT, MT, FC, and utility in the base case.

Li-ion battery has a higher capital cost compared with the other battery types, it will provide an acceptable saving value (18.75%) at 100% DOD because of its high efficiency and long lifetime. Hence, one can see that the total saving depends significantly on the lifetime and efficiency of the battery. Further, using the four battery types, the problem is also solved while considering various DOD values using the other optimization techniques, and the total operating cost obtained by GAMS and the other optimizers is shown in Fig. 9. Again, we can see that the total operating cost obtained by GAMS is the lowest compared to the other optimizers at all the considered DOD values.

3) ENERGY MANAGEMENT USING HALF-CHARGED BSSS: CASE 2

In case 2, the EM problem is solved in the GAMS environment using half-charged BSSs. Table 6 shows that the $PC_{battery}$, $ELTB_{DOD}$ and n_R will be the same as those obtained in case 1, but the SOC of the batteries during the day will differ, as illustrated in Fig. 10 for the NaS battery.

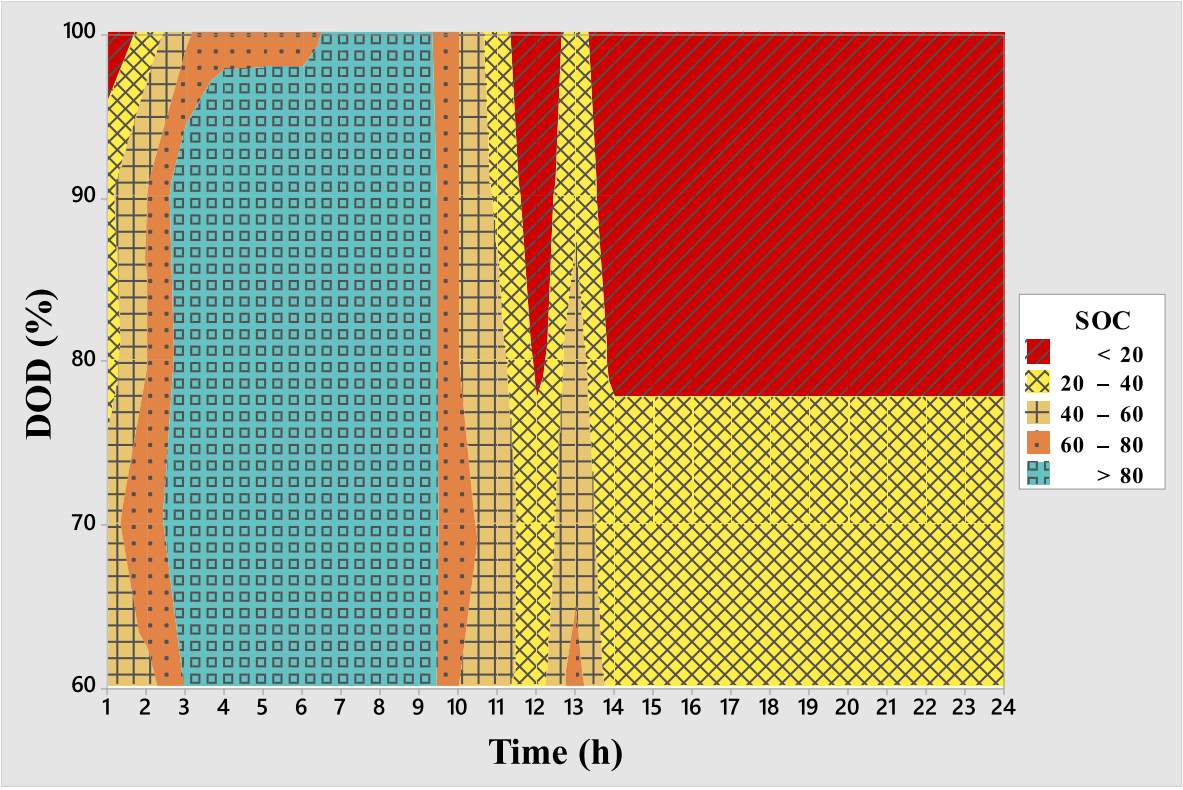

FIGURE 8. State of charge of the NaS battery versus DOD and time: case 1.

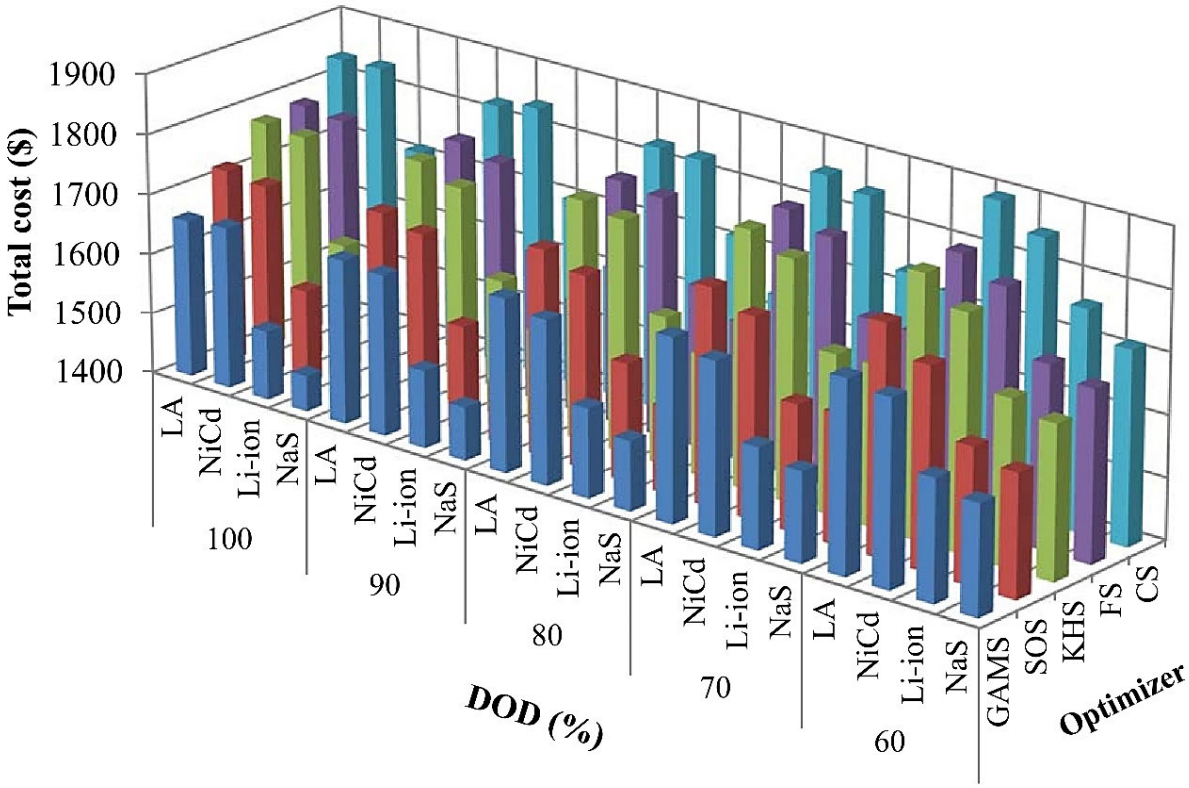

FIGURE 9. Total operating cost of the MG considering different DOD values: case 1.

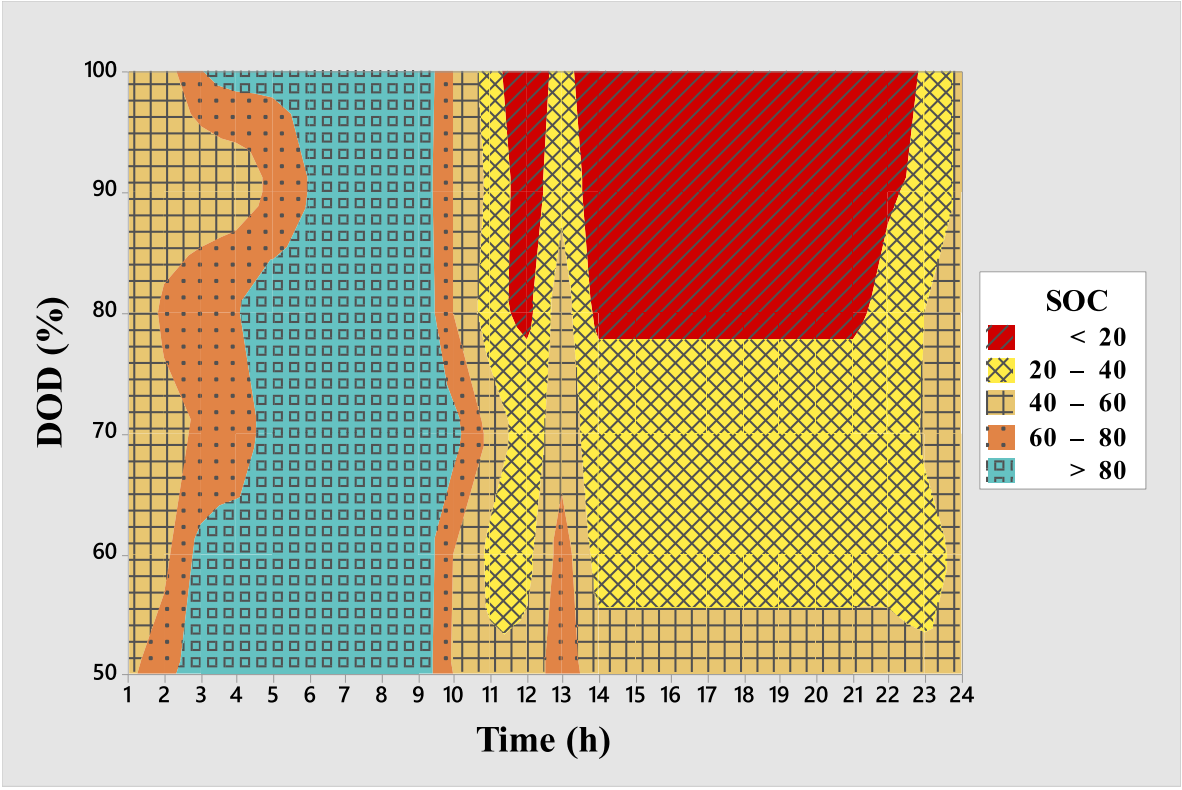

FIGURE 10. State of charge of NaS battery versus DOD and time: case 2.

TABLE 6. Numerical results obtained in case 2.

Case 2		$PC_{battery}$	$ELTB_{DOD}$	n_R	TIC_{BSS} ($)	Total cost per day ($)	$Saving$ (%)
BSS	DOD (%)						
LA	100	730	0.479	32	154.9	1660.5	10.82
	90	730	0.534	29	140.8	1677	9.94
	80	730	0.616	25	121.9	1685.6	9.47
	70	730	0.685	22	107.8	1700.5	8.67
	60	730	0.808	19	93.64	1715.4	7.87
	50	730	0.959	16	79.5	1730.3	7.07
NaS	100	730	5.479	3	27.5	**1458.8**	**21.65**
	90	730	6.85	3	27.5	1487.3	20.12
	80	730	8.219	2	20.5	1514.3	18.67
	70	730	9.589	2	20.5	1548.2	16.85
	60	730	12.329	2	20.5	1582.2	15.02
	50	730	13.699	2	20.5	1616.2	13.2
Li-ion	100	1095	2.74	6	89.1	1512.9	18.75
	90	1095	3.379	5	74.3	1526.9	17.99
	80	1095	4.109	4	59.4	1546.5	16.94
	70	1095	5.297	3	44.6	1566.1	15.89
	60	1095	6.301	3	44.6	1600.4	14.05
	50	1095	7.306	3	44.6	1634.8	12.2
NiCd	100	730	0.685	22	210.9	1667.3	10.45
	90	730	0.822	19	182.4	1665.7	10.54
	80	730	0.959	16	153.8	1669.5	10.33
	70	730	1.095	14	134.8	1682.8	9.62
	60	730	1.233	13	125.3	1705.7	8.39
	50	730	1.644	10	96.8	1709.5	8.19

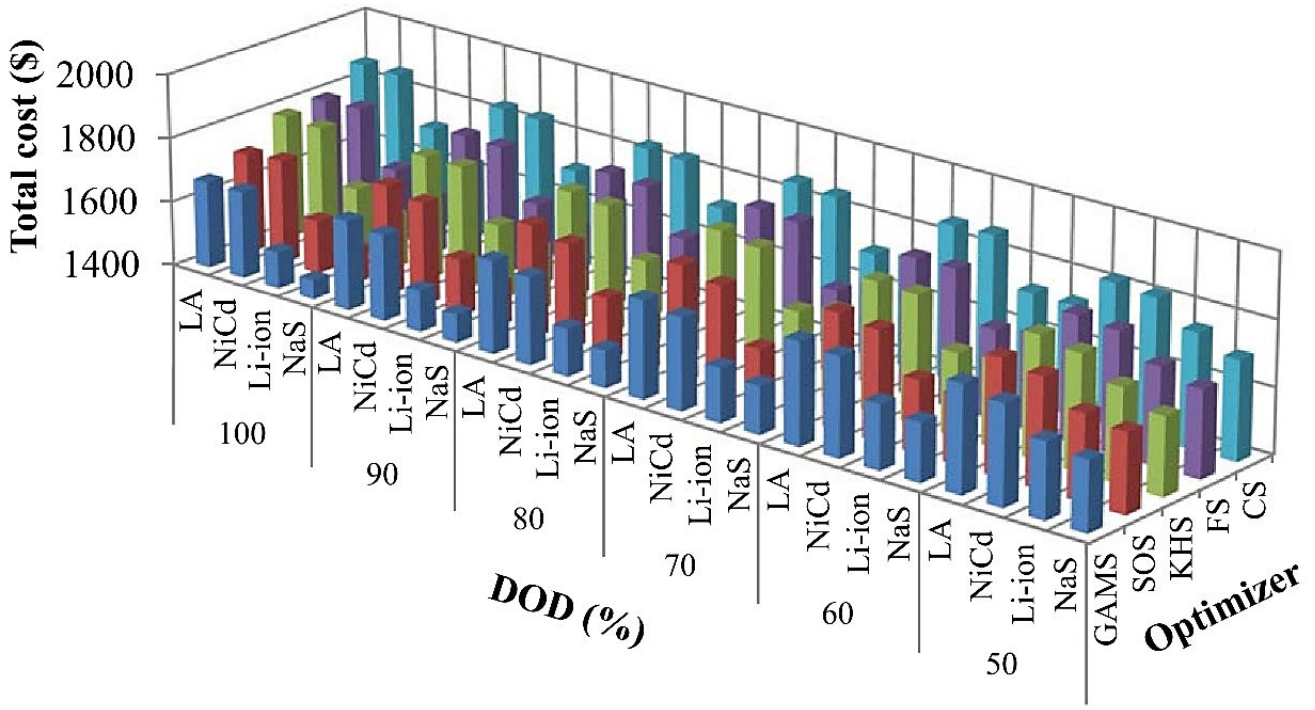

FIGURE 11. Total operation cost of the MG with various DOD values: case 2.

TABLE 7. Numerical results obtained in case 3.

Case 3		$PC_{battery}$	$ELTB_{DOD}$	n_R	TIC_{BSS} ($)	Total cost per day ($)	*Saving* (%)
BSS	DOD (%)						
LA	100	1095	0.3196	47	225.6	1779.4	4.44
	90	1095	0.356	43	206.7	1783.7	4.2
	80	1095	0.411	37	178.5	1778.7	4.47
	70	1095	0.457	33	159.6	1782.9	4.25
	60	1095	0.529	28	136	1782.4	4.27
	50	1095	0.639	24	117.2	1786.8	4.04
NaS	100	1095	3.653	5	41.5	**1505.1**	**19.17**
	90	1095	4.566	4	34.5	1522.3	18.24
	80	1095	5.479	3	27.5	1544.9	17.03
	70	1095	6.393	3	27.5	1574.4	15.44
	60	1095	8.219	2	20.5	1597.1	14.22
	50	1095	9.132	2	20.5	1627	12.62
Li-ion	100	1460	2.055	8	118.8	1573.5	15.49
	90	1460	2.534	6	89.1	1568.5	15.76
	80	1460	3.082	5	74.3	1583.8	14.94
	70	1460	3.973	4	59.4	1599.1	14.12
	60	1460	4.726	4	59.4	1629.3	12.5
	50	1460	5.479	3	44.6	1645.5	11.63
NiCd	100	1095	0.457	33	315.5	1809.7	2.81
	90	1095	0.548	28	268	1784.1	4.18
	80	1095	0.639	24	229.9	1773.5	4.75
	70	1095	0.731	21	201.4	1772.4	4.81
	60	1095	0.822	19	182.4	1780.9	4.36
	50	1095	1.096	14	134.8	1760.8	5.43

problem is also solved considering various DOD values using the other optimization techniques, and the total operating costs obtained by GAMS and the other optimizers are shown in Fig. 11. Again, we can see that the total operating cost obtained by GAMS is the lowest at all the considered DOD values.

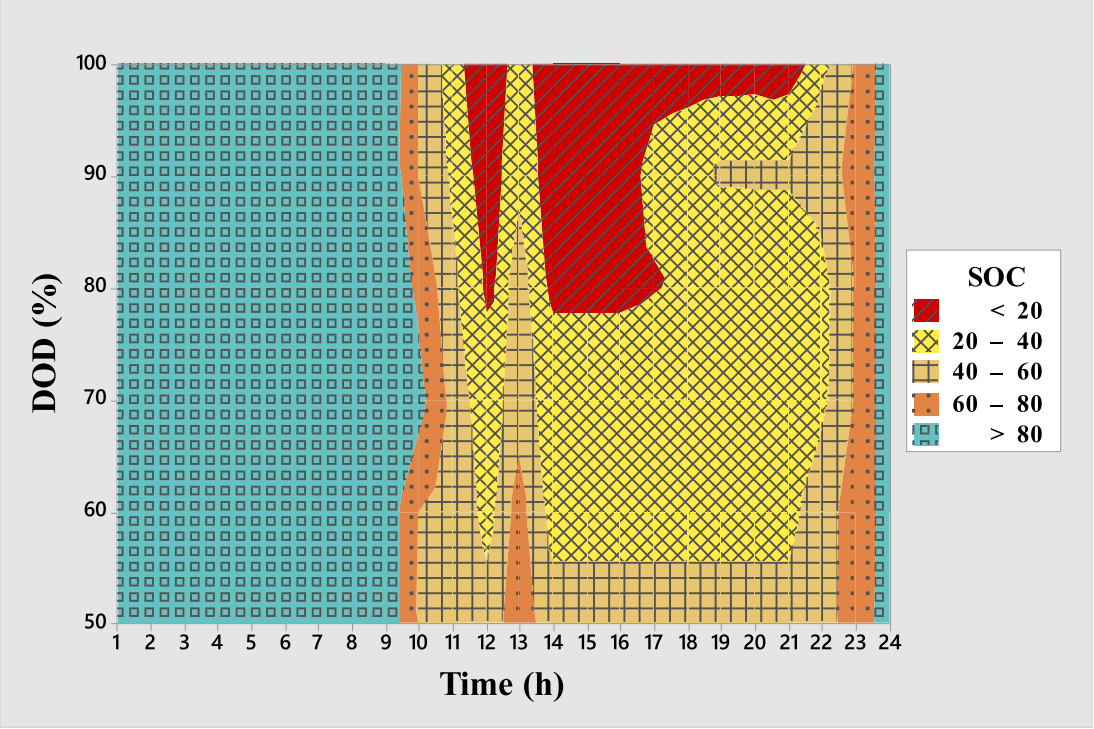

FIGURE 12. State of charge of NaS battery versus DOD and time: case 3.

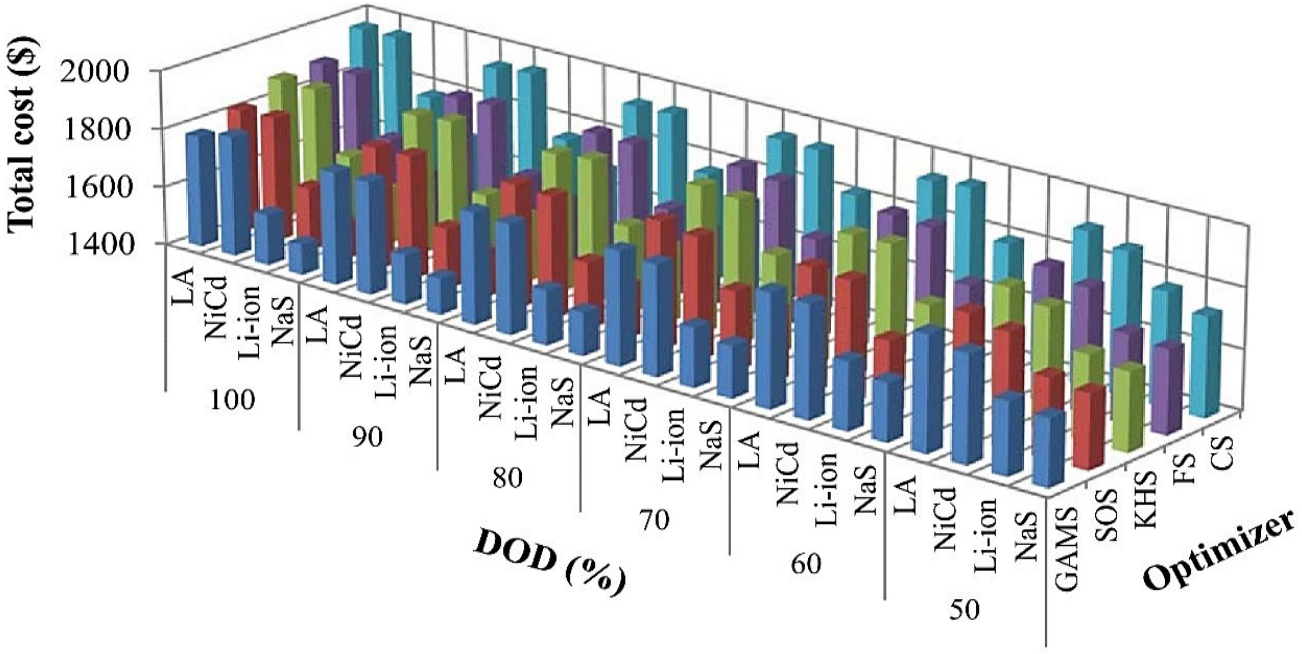

FIGURE 13. Total operation cost of the MG with various DOD values: case 3.

4) ENERGY MANAGEMENT USING FULLY CHARGED BSSS: CASE 3

In case 3, the EM is executed using initially fully charged BSSs and the results obtained are given in Table 7. Once more, the NaS battery provides the best results compared to the other batteries. Fig. 12 shows the variation of the SOC of the NaS battery versus the DOD and time during the day in case 3. As one can see, the output charge, discharge, and SOC of the batteries change considerably with the change of their initial charge.

The problem is solved using the other optimization techniques, and the total operating cost obtained by GAMS is

TABLE 8. The best results provided for each battery using the considered optimizers.

Optimizer	BSS	Cost ($)	DOD (%)	Initial charge		
				Zero	Half	Full
GAMS	LA	1660.5	100	√	X	X
	NaS	**1458.8**	100	√	√	X
	Li-ion	1512.9	100	√	√	X
	NiCd	1665.6	90	√	√	X
SOS	LA	1710.3	100	X	√	X
	NaS	1487.5	100	√	X	X
	Li-ion	1556.3	100	√	X	X
	NiCd	1708.2	90	√	X	X
KHS	LA	1775.9	100	X	√	X
	NaS	1527.5	100	√	X	X
	Li-ion	1607.3	100	√	X	X
	NiCd	1760.2	90	√	X	X
FS	LA	1781.3	100	√	X	X
	NaS	1536.2	100	√	X	X
	Li-ion	1626.1	100	√	X	X
	NiCd	1774.6	100	√	X	X
CS	LA	1829.7	90	√	X	X
	NaS	1586.7	100	√	X	X
	Li-ion	1707.4	90	√	X	X
	NiCd	1831.3	80	√	X	X

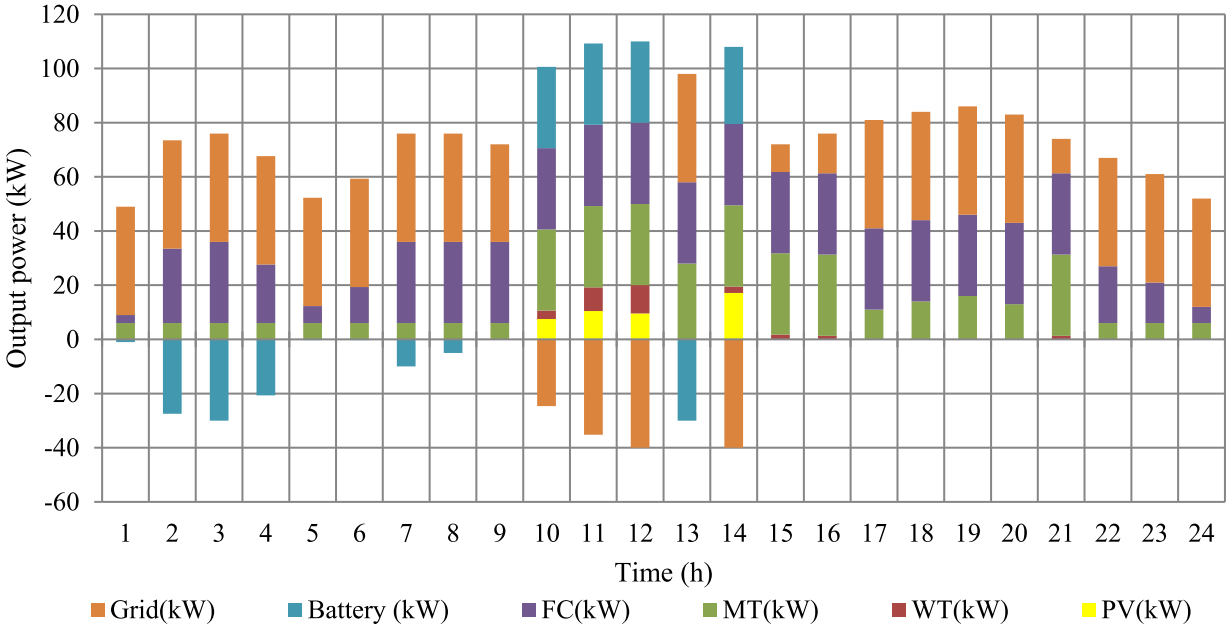

FIGURE 14. Optimal output powers of PV, BSS, WT, MT, FC, battery and utility at each hour during the day.

still the lowest compared to those obtained by the other optimizers at all the considered DOD values, as shown in Fig.13.

To sum up, Table 8 presents the minimum total operating cost of the MG obtained using the investigated optimizers among the four study cases. The total operating cost of the

TABLE 9. Five market price and their possibility of occurrence.

Time	Scenarios					Possibility of occurrence				
	S_1	S_2	S_3	S_4	S_5	S_1	S_2	S_3	S_4	S_5
1	0.2931	0.4216	0.3587	0.2247	0.1584	0.2122	0.1865	0.2061	0.1999	0.1953
2	0.2507	0.3730	0.3119	0.1873	0.1268	0.2122	0.1944	0.1994	0.2070	0.1870
3	0.2019	0.3071	0.2551	0.1508	0.1019	0.2046	0.1930	0.2071	0.2067	0.1886
4	0.1818	0.2707	0.2259	0.1362	0.0907	0.2078	0.1839	0.2053	0.2088	0.1943
5	0.1807	0.2708	0.2271	0.1353	0.0895	0.2034	0.1898	0.2040	0.2058	0.1969
6	0.2658	0.3921	0.3312	0.2000	0.1374	0.2174	0.1902	0.2035	0.2015	0.1874
7	0.2987	0.4240	0.3623	0.2345	0.1690	0.2062	0.1807	0.2056	0.2098	0.1977
8	0.4290	0.5856	0.5072	0.3501	0.2737	0.2086	0.1893	0.2136	0.2034	0.1852
9	2.2752	3.5270	2.9096	1.6600	1.0716	0.2089	0.1954	0.2042	0.2046	0.1869
10	6.0761	7.9099	7.0027	5.1521	4.2105	0.2113	0.1878	0.2021	0.2023	0.1966
11	6.0547	7.8988	6.9889	5.1236	4.2089	0.2049	0.1913	0.1999	0.2064	0.1975
12	6.0382	7.8986	6.9872	5.1266	4.1978	0.2059	0.1952	0.2042	0.2055	0.1892
13	2.3183	3.5342	2.9301	1.6797	1.0628	0.2115	0.1878	0.1979	0.2136	0.1892
14	6.0575	7.8911	6.9724	5.1070	4.1916	0.2008	0.1935	0.2031	0.2042	0.1984
15	2.6556	3.9201	3.2954	2.0036	1.3707	0.2037	0.1949	0.2027	0.2097	0.1890
16	2.3756	3.6279	3.0113	1.7349	1.0809	0.2037	0.1874	0.2062	0.2061	0.1967
17	0.5542	0.7649	0.6570	0.4534	0.3529	0.2105	0.1961	0.1981	0.2124	0.1829
18	0.4536	0.6068	0.5295	0.3769	0.3033	0.2105	0.1975	0.2051	0.1975	0.1894
19	0.3870	0.5290	0.4587	0.3189	0.2505	0.1994	0.1989	0.2122	0.1994	0.1901
20	0.4852	0.6370	0.5616	0.4111	0.3336	0.2039	0.1937	0.2100	0.2066	0.1857
21	2.3507	3.6132	2.9847	1.7168	1.1146	0.2054	0.2019	0.2068	0.2016	0.1842
22	0.5855	0.7195	0.6524	0.5162	0.4507	0.2057	0.1905	0.2111	0.2048	0.1879
23	0.3666	0.5090	0.4381	0.2943	0.2219	0.2147	0.1808	0.2023	0.2115	0.1906
24	0.3268	0.4532	0.3913	0.2619	0.1978	0.2039	0.1897	0.2007	0.2068	0.1989

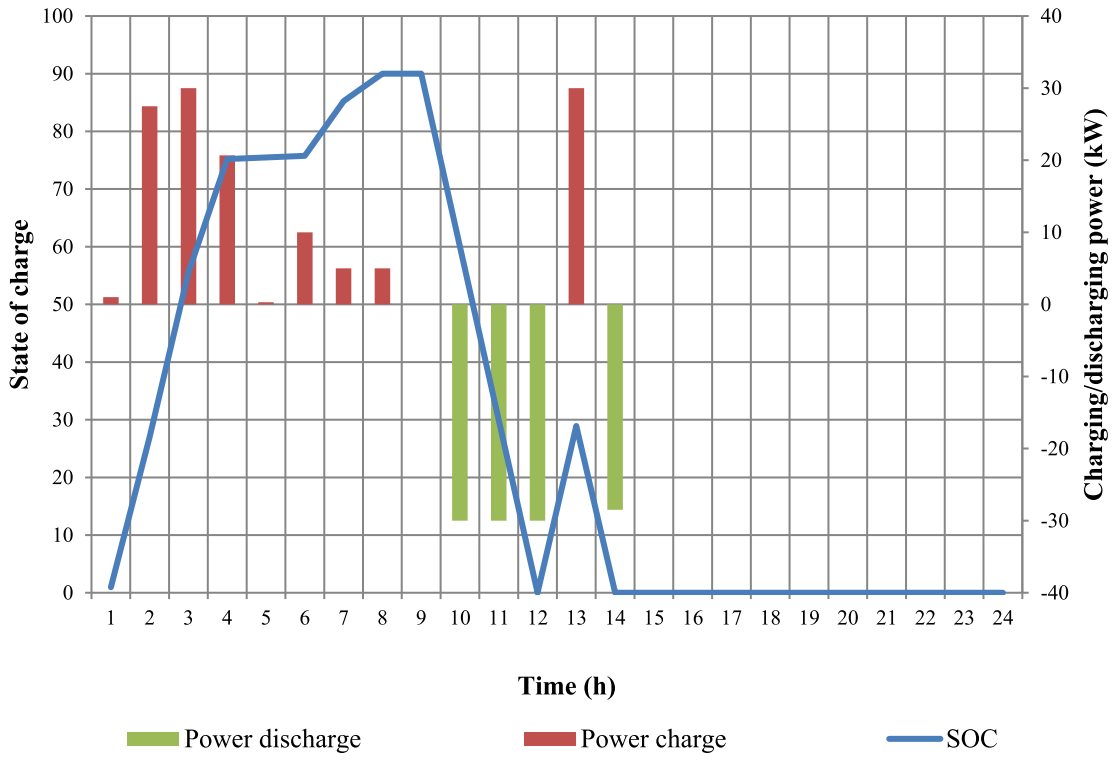

FIGURE 15. State of charge and charging/discharging schedule of the NaS battery: deterministic case.

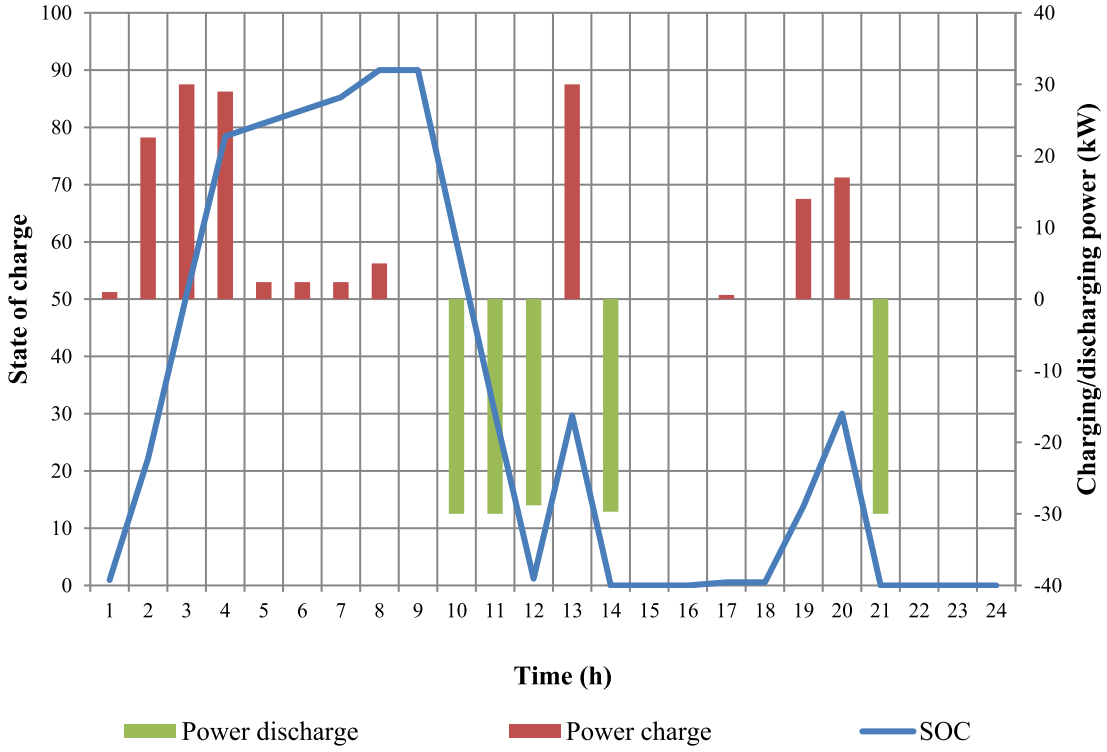

FIGURE 16. State of charge and charging/discharging schedule of the NaS battery: stochastic case.

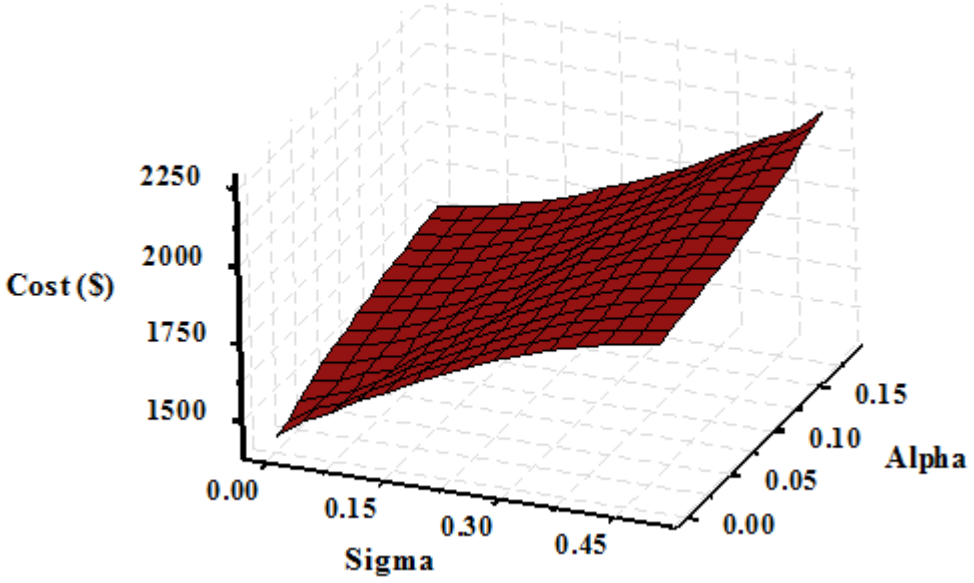

FIGURE 17. Optimum robustness function value versus cost deviation factor and the total operating cost of the MG.

MG is reduced from $1861.57 per day (with no BSS) to $1458.8 per day using the NaS battery, which means a total saving of 21.6% at a DOD of 100%. Using this result, the optimal output powers obtained by GAMS of the BSS, PV, WT, MT, FC, and utility at each hour during the day are shown in Fig. 14.

B. STOCHASTIC SOLUTION WITH UNCERTAIN MARKET PRICE

In the optimization, we utilized the five scenarios presented in Table 9, which is obtained by the FCM technique to characterize the variation of the market price. The possibility of occurrence of each scenario at each hour is also presented

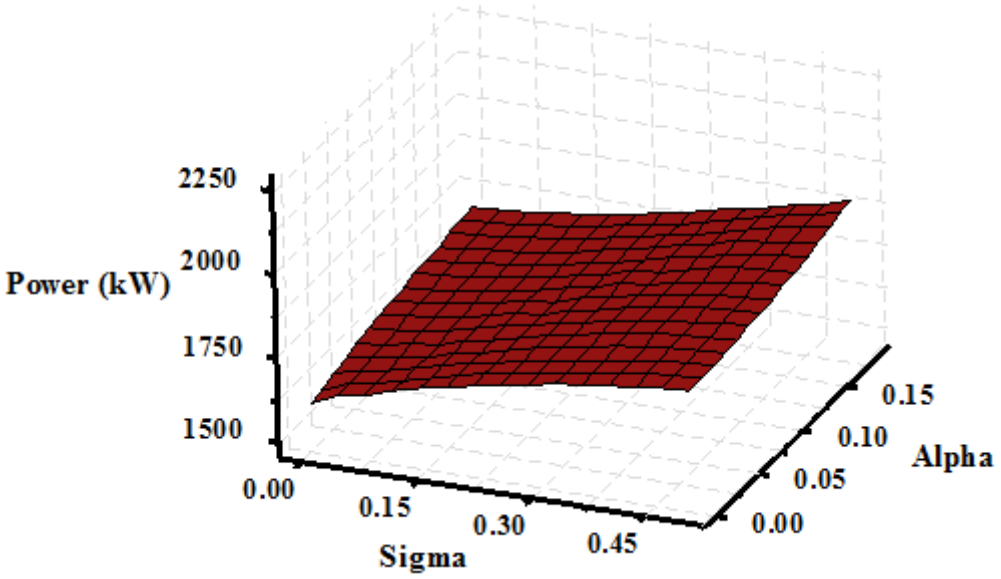

FIGURE 18. Optimum robustness function value versus cost deviation factor and the total generated power of the MG.

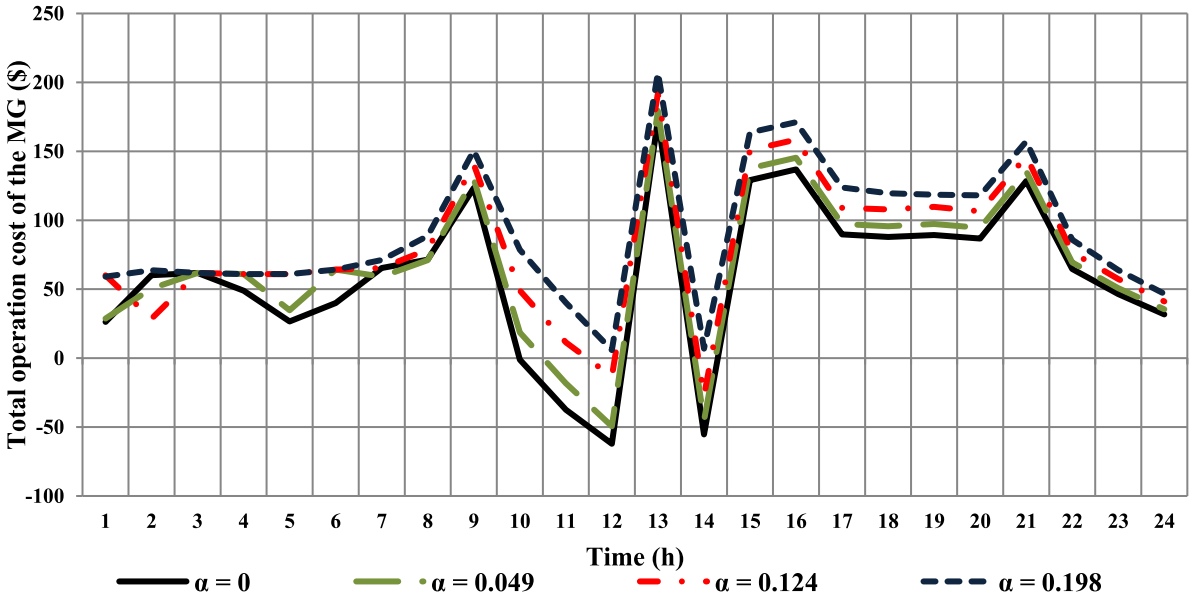

FIGURE 19. Hourly operation cost of MG considering different robustness function values.

in Table 11. Then, the problem is solved using GAMS: MINLP DICOPT solver with a zero-charged NaS battery considered at 100% DOD, which represents the best solution achieved in the deterministic case.

Figs. 15 and 16 show the SOC and the charging/discharging schedule of the NaS battery in both the deterministic and stochastic cases, respectively.

Although the number of cycles performed by the NaS battery increased from 730 to 1095 cycles per year and the number of replacements of the battery also increased from three to five times during the lifetime of the project, the total operating cost of the MG obtained in the stochastic case is $1406.7, which is 3.6% lower than that achieved in the deterministic case. We can also see from Figs. 15 and 16 that the charging/discharging schedule of the NaS battery obtained in the stochastic case is slightly different from that obtained in the deterministic case. For instance, in the first period, from hour 1 to hour 8, the NaS battery is charging because the energy market price is low, and the total load is not high. The values of power charged in the stochastic case vary from that shown in the deterministic case based on the values of the market energy price and the generation and total load constraints during the day. Further, during the period from hour 10 to hour 12 and at hour 14, the value of the energy market price is high; thus, the NaS battery is discharging during these periods but with different schedules in the determin-

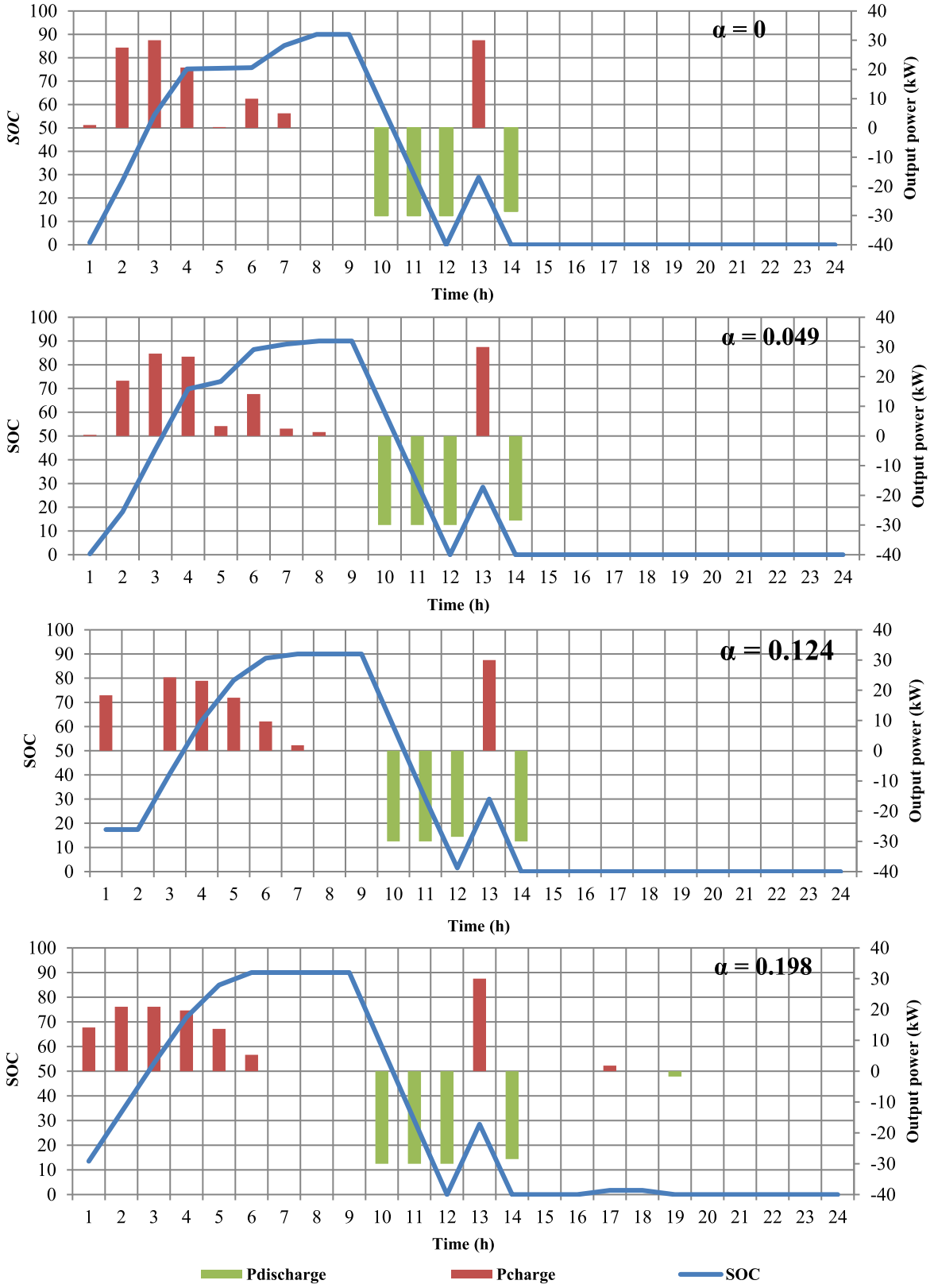

FIGURE 20. The state of charge and charging/discharging schedule of the NaS battery considering different robustness function values.

istic and stochastic cases. In the stochastic case, the NaS battery is charging during the period from hour 17 to 20, and then it is discharging at hour 21 because the energy market price at hour 21 is higher than the price in the deterministic case.

C. SOLUTION OF THE ROBUST OPTIMIZATION MODEL WITH AN UNCERTAIN LOAD PROFILE

The MGCC is responsible for making a particular schedule of the power imported from or exported to the grid, the output power of each DG, and charging/discharge of BSS, to minimize the operating cost of the MG. In this work, the model of the MGCC is risk-based over a day's scheduling period due to load uncertainty. Therefore, a robust optimization technique is employed to obtain the most economic hourly operation of the studied MG and protect MGCC decisions against high costs, in which the IGDT is used to model the risk of load uncertainty and then to provide more robustness to the MGCC decisions by utilizing the available load forecast in a method where a maximum suitable operation cost of the MG is always guaranteed.

In this respect, (42) is solved to get the optimum values of the robustness function represented by α for different values of σ using GAMS: MINLP, DICOPT solver. The minimum cost (C_o) is decided as the best value obtained from the deterministic problem solution, i.e. C_o is \$1458.8 for the deterministic case. Fig. 17 shows the optimum values of α and the resulting total operating cost for different values of σ, starting from 0 to 0.5 with a step set to 0.05. Also, Fig. 18 shows the optimum values of α and the total generated power of the MG for the same values of σ. Each value of σ signifies a different C_c value. For instance, the C_c value equals \$1969.38 when $\sigma = 0.35$, i.e., the total operating cost of the MG will not be higher than \$1969.38 in such a case. Likewise, if σ equals 0.5, the C_c value will equal \$2188.2.

We can see from Figs. 17 and 18 that the value of α that gives the solution of the deterministic optimization is zero. Further, the optimum value of α will increase as σ increases. Additionally, both the total operating cost and the total generated power of the MG increase with the increase of σ and α. Fig. 19 shows the hourly total operating cost of the MG at different α values.

The value of the total operating cost at a specific value of α is considered the highest cost; that is, for a given risk level, the total operating cost of the MG would be less than the obtained value.

Fig. 20 shows the SOC and the charging/discharging schedule of the NaS battery, considering different values of α. When α increases, the total load will increase and the operation of the MG will change. Accordingly, the hourly economic schedule of the battery will change. Fig. 20 shows that the charging schedule of the NaS battery in the first period (from hour 1 to hour 8) would be changed depending on the value of α to achieve the maximum benefits from the battery by considering the generation, load, and battery constraints.

At all values of α, the battery discharging schedule is at the periods from hour 10 to hour 12 and at hour 14 because the energy market price is significantly high in these periods.

V. CONCLUSION

A comparison study of the economical EM of a grid-connected MG was presented in this study. The objective function was to minimize the total operating cost of the MG. Different BSS technologies with several initial charge possibilities and DOD values are taken into account in this work, in addition to the variation of the energy market price and electrical loads uncertainty. The results obtained show that the total operating cost of the MG can be reduced considerably when a BSS is integrated into the MG. We outlined the main findings of this study as follows: (1) the total cost per day of the BSS through the lifetime of the project decreases when the value of DOD increases; however, this may not lead to a reduction of the total operating cost because of the other factors that affect the operation, such as the charging/discharging schedule of the BSS, output power of each DG, and power imported from or exported to the main grid; (2) among the different BSS technologies, the impact of NaS batteries in the reduction of total operating cost of MG is clearer than the other BSS batteries due to their high efficiency and long life time, which resulted in a reduction in the total operating cost from \$1861.57 per day (with no BSS) to \$1458.8 per day, a total daily saving of 21.6%; (3) although lead acid batteries have a lower capital cost compared with the other batteries, this results in a high total operating cost due to their low efficiency and short life time; (4) the total cost saving depends substantially on the lifetime and efficiency of the battery; (5) the initial charge of the BSS affects the charging/discharging schedule of the BSS, and consequently changes the output power of each DG, and the power imported from or exported to the main grid to achieve the minimum objective function; (6) the variation of the energy market price is modeled by the stochastic optimization to obtain the actual results, and the total operating cost of the MG obtained was \$1406.7, which is 3.6% lower than that achieved in the deterministic case; (7) it was also concluded that deterministic studies that ignore the uncertainty of parameters result in conservative results that usually lead to a noticeable overestimation of the costs; (8) a robust optimization technique is employed to obtain the most economic hourly operation of the studied MG and protect the MGCC decisions against high costs, in which the IGDT is used to model the risk of load uncertainty and then to provide more robustness to the MGCC decisions by utilizing the available load forecast in a method where a maximum suitable operation cost of the MG can always be guaranteed using the best results obtained in the deterministic case; (9) the performance of GAMS in all cases was better than the performance of other optimization techniques such as SOS, KHS, FS, and CS. Finally, a factor that was beyond the framework of the study, and will be included in future studies, is the techno-environmental concern to minimize the emissions of the MG along with the total operating cost, taking into account various uncertain parameters and high penetration of renewables.

REFERENCES

[1] S. M. Ismael, S. H. E. Abdel Aleem, A. Y. Abdelaziz, and A. F. Zobaa, "State-of-the-art of hosting capacity in modern power systems with distributed generation," *Renew. Energy*, vol. 130, pp. 1002–1020, Jan. 2019.

[2] K. Milis, H. Peremans, and S. Van Passel, "The impact of policy on microgrid economics: A review," *Renew. Sustain. Energy Rev.*, vol. 81, pp. 3111–3119, Jan. 2018.

[3] C. A. Alvez, J. E. Sarmiento, A. C. Z. de Souza, P. F. Ribeiro, R. C. Leme, and A. Fiorese, "Energy management of microgrids including frequency and voltage restoration," in *Proc. IEEE Power Energy Soc. Gen. Meeting (PESGM)*, Aug. 2018, pp. 1–5.

[4] A. Abdalrahman and W. Zhuang, "PEV charging infrastructure siting based on spatial–temporal traffic flow distribution," *IEEE Trans. Smart Grid*, vol. 10, no. 6, pp. 6115–6125, Nov. 2019.

[5] F. D. González, A. Sumper, and O. G. Bellmunt, *Energy Storage in Power Systems*, 1st ed. Hoboken, NJ, USA: Wiley, 2016.

[6] Y. M. Alsmadi, A. M. Abdel-hamed, A. E. Ellissy, A. S. El-Wakeel, A. Y. Abdelaziz, V. Utkin, and A. A. Uppal, "Optimal configuration and energy management scheme of an isolated micro-grid using cuckoo search optimization algorithm," *J. Franklin Inst.*, vol. 356, no. 8, pp. 4191–4214, May 2019.

[7] N. Bazmohammadi, A. Tahsiri, A. Anvari-Moghaddam, and J. M. Guerrero, "Stochastic predictive control of multi-microgrid systems," *IEEE Trans. Ind. Appl.*, vol. 55, no. 5, pp. 5311–5319, Sep. 2019.

[8] M. Vahedipour-Dahraie, H. Rashidizadeh-Kermani, A. Anvari-Moghaddam, and J. M. Guerrero, "Stochastic risk-constrained scheduling of renewable-powered autonomous microgrids with demand response actions: Reliability and economic implications," *IEEE Trans. Ind. Appl.*, vol. 56, no. 2, pp. 1882–1895, Mar. 2019.

[9] W. Du, L. Yao, D. Wu, X. Li, G. Liu, and T. Yang, "Accelerated distributed energy management for microgrids," in *Proc. IEEE Power Energy Soc. Gen. Meeting (PESGM)*, Aug. 2018, pp. 1–5.

[10] A. Kaur, J. Kaushal, and P. Basak, "A review on microgrid central controller," *Renew. Sustain. Energy Rev.*, vol. 55, pp. 338–345, Mar. 2016.

[11] F. Delfino, G. Ferro, R. Minciardi, M. Robba, M. Rossi, and M. Rossi, "Identification and optimal control of an electrical storage system for microgrids with renewables," *Sustain. Energy, Grids Netw.*, vol. 17, Mar. 2019, Art. no. 100183.

[12] J. Liu, G. Rizzoni, and B. Yurkovich, "Stochastic energy management for microgrids with constraints under uncertainty," in *Proc. IEEE Transp. Electrific. Conf. Expo (ITEC)*, Jun. 2016, pp. 1–6.

[13] H. Balakrishnan, K. K. S. Tomar, and S. N. Singh, "An agent based approach for efficient energy management of microgrids," in *Proc. IEEE Region 10 Symp. (TENSYMP)*, Jul. 2017, pp. 1–5.

[14] H. Mehrjerdi, E. Rakhshani, and A. Iqbal, "Substation expansion deferral by multi-objective battery storage scheduling ensuring minimum cost," *J. Energy Storage*, vol. 27, Feb. 2020, Art. no. 101119.

[15] I. Alsaidan, A. Khodaei, and W. Gao, "A comprehensive battery energy storage optimal sizing model for microgrid applications," *IEEE Trans. Power Syst.*, vol. 33, no. 4, pp. 3968–3980, Jul. 2018.

[16] H. Mehrjerdi, "Simultaneous load leveling and voltage profile improvement in distribution networks by optimal battery storage planning," *Energy*, vol. 181, pp. 916–926, Aug. 2019.

[17] A. J. Crawford, Q. Huang, M. C. W. Kintner-Meyer, J.-G. Zhang, D. M. Reed, V. L. Sprenkle, V. V. Viswanathan, and D. Choi, "Lifecycle comparison of selected Li-ion battery chemistries under grid and electric vehicle duty cycle combinations," *J. Power Sources*, vol. 380, pp. 185–193, Mar. 2018.

[18] W. Jing, C. H. Lai, D. K. X. Ling, W. S. H. Wong, and M. L. D. Wong, "Battery lifetime enhancement via smart hybrid energy storage plug-in module in standalone photovoltaic power system," *J. Energy Storage*, vol. 21, pp. 586–598, Feb. 2019.

[19] D. Wang, J. Qiu, L. Reedman, K. Meng, and L. L. Lai, "Two-stage energy management for networked microgrids with high renewable penetration," *Appl. Energy*, vol. 226, pp. 39–48, Sep. 2018.

[20] C. K. Nayak, K. Kasturi, and M. R. Nayak, "Economical management of microgrid for optimal participation in electricity market," *J. Energy Storage*, vol. 21, pp. 657–664, Feb. 2019.

[21] M. A. Hossain, H. R. Pota, S. Squartini, and A. F. Abdou, "Modified PSO algorithm for real-time energy management in grid-connected microgrids," *Renew. Energy*, vol. 136, pp. 746–757, Jun. 2019.

[22] M. A. Hossain, H. R. Pota, S. Squartini, F. Zaman, and K. M. Muttaqi, "Energy management of community microgrids considering degradation cost of battery," *J. Energy Storage*, vol. 22, pp. 257–269, Apr. 2019.

[23] M. Abedini, M. H. Moradi, and S. M. Hosseinian, "Optimal management of microgrids including renewable energy scources using GPSO-GM algorithm," *Renew. Energy*, vol. 90, pp. 430–439, May 2016.

[24] T. Iqbal, Z. Khitab, F. Girbau, and A. Sumper, "Energy management system for optimal operatioin of microgrids network," in *Proc. IEEE Int. Conf. Smart Energy Grid Eng. (SEGE)*, Aug. 2018, pp. 68–72.

[25] M. Ruiz-Cortés, E. González-Romera, R. Amaral-Lopes, E. Romero-Cadaval, J. Martins, M. I. Milanés-Montero, and F. Barrero-González, "Optimal charge/discharge scheduling of batteries in microgrids of prosumers," *IEEE Trans. Energy Convers.*, vol. 34, no. 1, pp. 468–477, Mar. 2019.

[26] A. Fathy and A. Y. Abdelaziz, "Single and multi-objective operation management of micro-grid using krill herd optimization and ant lion optimizer algorithms," *Int. J. Energy Environ. Eng.*, vol. 9, no. 3, pp. 257–271, Sep. 2018.

[27] M. Sedighizadeh, M. Esmaili, A. Jamshidi, and M.-H. Ghaderi, "Stochastic multi-objective economic-environmental energy and reserve scheduling of microgrids considering battery energy storage system," *Int. J. Electr. Power Energy Syst.*, vol. 106, pp. 1–16, Mar. 2019.

[28] M. H. Moradi and M. Eskandari, "A hybrid method for simultaneous optimization of DG capacity and operational strategy in microgrids considering uncertainty in electricity price forecasting," *Renew. Energy*, vol. 68, pp. 697–714, Aug. 2014.

[29] H. Fan, Q. Yuan, and H. Cheng, "Multi-objective stochastic optimal operation of a grid-connected microgrid considering an energy storage system," *Appl. Sci.*, vol. 8, no. 12, p. 2560, Dec. 2018.

[30] A. Narayan and K. Ponnambalam, "Risk-averse stochastic programming approach for microgrid planning under uncertainty," *Renew. Energy*, vol. 101, pp. 399–408, Feb. 2017.

[31] M. Tavakkoli, E. Pouresmaeil, R. Godina, I. Vechiu, and J. P. S. Catalão, "Optimal management of an energy storage unit in a PV-based microgrid integrating uncertainty and risk," *Appl. Sci.*, vol. 9, no. 1, p. 169, Jan. 2019.

[32] T. Rui, G. Li, Q. Wang, C. Hu, W. Shen, and B. Xu, "Hierarchical optimization method for energy scheduling of multiple microgrids," *Appl. Sci.*, vol. 9, no. 4, p. 624, Feb. 2019.

[33] S. Mazzola, C. Vergara, M. Astolfi, V. Li, I. Perez-Arriaga, and E. Macchi, "Assessing the value of forecast-based dispatch in the operation of off-grid rural microgrids," *Renew. Energy*, vol. 108, pp. 116–125, Aug. 2017.

[34] L. Mellouk, M. Ghazi, A. Aaroud, M. Boulmalf, D. Benhaddou, and K. Zine-Dine, "Design and energy management optimization for hybrid renewable energy system-case study: Laayoune region," *Renew. Energy*, vol. 139, pp. 621–634, Aug. 2019.

[35] M. A. M. Ramli, H. R. E. H. Bouchekara, and A. S. Alghamdi, "Optimal sizing of PV/wind/diesel hybrid microgrid system using multi-objective self-adaptive differential evolution algorithm," *Renew. Energy*, vol. 121, pp. 400–411, Jun. 2018.

[36] M. Esmaili, H. Shafiee, and J. Aghaei, "Range anxiety of electric vehicles in energy management of microgrids with controllable loads," *J. Energy Storage*, vol. 20, pp. 57–66, Dec. 2018.

[37] L. Igualada, C. Corchero, M. Cruz-Zambrano, and F.-J. Heredia, "Optimal energy management for a residential microgrid including a Vehicle-to-Grid system," *IEEE Trans. Smart Grid*, vol. 5, no. 4, pp. 2163–2172, Jul. 2014.

[38] J. Yan, M. Menghwar, E. Asghar, M. Kumar Panjwani, and Y. Liu, "Real-time energy management for a smart-community microgrid with battery swapping and renewables," *Appl. Energy*, vol. 238, pp. 180–194, Mar. 2019.

[39] T. Alharbi and K. Bhattacharya, "Optimal scheduling of energy resources and management of loads in isolated/islanded microgrids," *Can. J. Elect. Comput. Eng.*, vol. 40, no. 4, pp. 284–294, 2017.

[40] E. Mortaz and J. Valenzuela, "Microgrid energy scheduling using storage from electric vehicles," *Electric Power Syst. Res.*, vol. 143, pp. 554–562, Feb. 2017.

[41] X. Lu, K. Zhou, and S. Yang, "Multi-objective optimal dispatch of microgrid containing electric vehicles," *J. Cleaner Prod.*, vol. 165, pp. 1572–1581, Nov. 2017.

[42] V. N. Coelho, I. M. Coelho, B. N. Coelho, M. W. Cohen, A. J. R. Reis, S. M. Silva, M. J. F. Souza, P. J. Fleming, and F. G. Guimarães, "Multi-objective energy storage power dispatching using plug-in vehicles in a smart-microgrid," *Renew. Energy*, vol. 89, pp. 730–742, Apr. 2016.

[43] S. Esmaeili, A. Anvari-Moghaddam, and S. Jadid, "Optimal operation scheduling of a microgrid incorporating battery swapping stations," *IEEE Trans. Power Syst.*, vol. 34, no. 6, pp. 5063–5072, Nov. 2019.
[44] S. Sharma, S. Bhattacharjee, and A. Bhattacharya, "Grey wolf optimisation for optimal sizing of battery energy storage device to minimise operation cost of microgrid," *IET Gener., Transmiss. Distrib.*, vol. 10, no. 3, pp. 625–637, Feb. 2016.
[45] B. Bahmani-Firouzi and R. Azizipanah-Abarghooee, "Optimal sizing of battery energy storage for micro-grid operation management using a new improved bat algorithm," *Int. J. Elect. Power Energy Syst.*, vol. 56, pp. 42–54, Mar. 2014.
[46] M. H. Mostafa, S. G. Ali, S. H. E. A. Aleem, and A. Y. Abdelaziz, "Optimal allocation of energy storage system for improving performance of microgrid using symbiotic organisms search," in *Proc. 20th Int. Middle East Power Syst. Conf. (MEPCON)*, Dec. 2018, pp. 474–479.
[47] T. Kerdphol, Y. Qudaih, and Y. Mitani, "Optimum battery energy storage system using PSO considering dynamic demand response for microgrids," *Int. J. Elect. Power Energy Syst.*, vol. 83, pp. 58–66, Dec. 2016.
[48] A. F. Zobaa, S. H. E. A. Aleem, and A. Y. Abdelaziz, *Classical and Recent Aspects of Power System Optimization*. Amsterdam, The Netherlands: Elsevier, 2018.
[49] M. Jabir, H. Mokhlis, M. A. Muhammad, and H. A. Illias, "Optimal battery and fuel cell operation for energy management strategy in MG," *IET Gener., Transmiss. Distrib.*, vol. 13, no. 7, pp. 997–1004, Apr. 2019.
[50] A. M. Azmy and I. Erlich, "Online optimal management of PEM fuel cells using neural networks," *IEEE Trans. Power Del.*, vol. 20, no. 2, pp. 1051–1058, Apr. 2005.
[51] A. Giugno, A. Cuneo, and A. Traverso, "Analysis of uncertainties in compact plate-fin recuperators for microturbines," *Appl. Thermal Eng.*, vol. 150, pp. 1243–1251, Mar. 2019.
[52] Z. Salameh, *Renewable Energy System Design: Renew Energy and Alternative Technologies*, 1st ed. New York, NY, USA: Academic, 2014.
[53] A. Zakaria, F. B. Ismail, M. S. H. Lipu, and M. A. Hannan, "Uncertainty models for stochastic optimization in renewable energy applications," *Renew. Energy*, vol. 145, pp. 1543–1571, Jan. 2020.
[54] J. C. Dunn, "A fuzzy relative of the ISODATA process and its use in detecting compact well-separated clusters," *J. Cybern.*, vol. 3, no. 3, pp. 32–57, Jan. 1973.
[55] J. C. Bezdek, *Pattern Recognition with Fuzzy Objective Function Algorithms*. New York, NY, USA: Plenum Press, 1981.
[56] T. Yu, J. Yang, and W. Lu, "Dynamic background subtraction using histograms based on fuzzy C-Means clustering and fuzzy nearness degree," *IEEE Access*, vol. 7, pp. 14671–14679, 2019.
[57] W. Zang, Z. Wang, D. Jiang, and X. Liu, "A kernel-based intuitionistic fuzzy C-means clustering using improved multi-objective immune algorithm," *IEEE Access*, vol. 7, pp. 84565–84579, 2019.
[58] A. Soroudi, A. Rabiee, and A. Keane, "Information gap decision theory approach to deal with wind power uncertainty in unit commitment," *Electric Power Syst. Res.*, vol. 145, pp. 137–148, Apr. 2017.
[59] M. Majidi, B. Mohammadi-Ivatloo, and A. Soroudi, "Application of information gap decision theory in practical energy problems: A comprehensive review," *Appl. Energy*, vol. 249, pp. 157–165, Sep. 2019.
[60] E. Shi, F. Jabari, A. Anvari-Moghaddam, M. Mohammadpourfard, and B. Mohammadi-ivatloo, "Risk-constrained optimal chiller loading strategy using information gap decision theory," *Appl. Sci.*, vol. 9, no. 9, p. 1925, 2019.
[61] A. Khazali, N. Rezaei, A. Ahmadi, and B. Hredzak, "Information gap decision theory based preventive/corrective voltage control for smart power systems with high wind penetration," *IEEE Trans Ind. Informat.*, vol. 14, no. 10, pp. 4385–4394, Oct. 2018.
[62] F. Benhamida, I. Ziane, S. Souag, Y. Salhi, and B. Dehiba, "A quadratic programming optimization for dynamic economic load dispatch: Comparison with GAMS," in *Proc. 3rd Int. Conf. Syst. Control*, Oct. 2013, pp. 625–630.
[63] R. Singh and A. Kumar S. M., "Estimation of off shore wind power potential and cost optimization of wind farm in Indian coastal region by using GAMS," in *Proc. Int. Conf. Current Trends Towards Converging Technol. (ICCTCT)*, Mar. 2018, pp. 1–6.
[64] T. Ha, Y. Zhang, J. Hao, V. Thang, C. Li, and Z. Cai, "Energy Hub's structural and operational optimization for minimal energy usage costs in energy systems," *Energies*, vol. 11, no. 4, p. 707, Mar. 2018.
[65] M. K. Amosa and T. Majozi, "GAMS supported optimization and predictability study of a multi-objective adsorption process with conflicting regions of optimal operating conditions," *Comput. Chem. Eng.*, vol. 94, pp. 354–361, Nov. 2016.
[66] A. Rabiee, M. Sadeghi, and J. Aghaei, "Modified imperialist competitive algorithm for environmental constrained energy management of microgrids," *J. Cleaner Prod.*, vol. 202, pp. 273–292, Nov. 2018.

MOSTAFA H. MOSTAFA received the B.Sc. and M.Sc. degrees in electrical power and machines from the Faculty of Engineering, Cairo University, Egypt, in 2012 and 2016, respectively. He is currently pursuing the Ph.D. degree with the Electrical Power and Machines Department, Faculty of Engineering, Ain Shams University. He is also an Assistant Teacher with the International Academy for Engineering and Media Science. His research interests include energy management, distributed generation, renewable energy technologies, optimization, and energy storage systems.

SHADY H. E. ABDEL ALEEM (Member, IEEE) received the B.Sc. degree in electrical power and machines from the Faculty of Engineering, Helwan University, Egypt, in 2002, and the M.Sc. and Ph.D. degrees in electrical power and machines from the Faculty of Engineering, Cairo University, Egypt, in 2010 and 2013, respectively. Since September 2018, he has been an Associate Professor with the 15th of May Higher Institute of Engineering. He is the author or coauthor of many refereed journal and conference papers. He has published more than 90 journal and conference papers, fifteen book chapters, and six edited books with the Institution of Engineering and Technology (IET), Elsevier, Springer, and InTech publishers. His research interests include harmonic problems in power systems, power quality, renewable energy, smart grid, energy efficiency, decision making, optimization, green energy, and economics.

Dr. Aleem is a member of the Institution of Engineering and Technology (IET). He was awarded the State Encouragement Award in Engineering Sciences from Egypt, in 2017. He is an Editor/Associate Editor of *International Journal of Renewable Energy Technology, International Journal of Electrical Engineering and Education*, and *Vehicle Dynamics*.

SAMIA G. ALI received the B.Sc. degree in electrical power and machines from the Faculty of Engineering, Zagazig University, Egypt, in 1988, the M.Sc. degree from Mansoura University, Egypt, in 2000, and the Ph.D. degree from Ain-Shams University, Egypt, in 2006. She is currently an Assistant Professor with the Faculty of Engineering, Kafrelsheikh University, Egypt, and also an adjunct Assistant Professor with the International Academy for Engineering and Media Science, Egypt. Her research interests include energy management, machine, renewable energy technologies, smart grid, and power system planning.

ALMOATAZ Y. ABDELAZIZ (Senior Member, IEEE) received the B.Sc. and M.Sc. degrees in electrical engineering from Ain Shams University, Cairo, Egypt, in 1985 and 1990, respectively, and the Ph.D. degree in electrical engineering according to the channel system between Ain Shams University, Egypt, and Brunel University, U.K., in 1996. He has been a Professor of electrical power engineering with Ain Shams University, since 2007. He has authored or coauthored more than 400 refereed journal and conference papers, 25 book chapters, and three edited books with Elsevier and Springer. His research areas include the applications of artificial intelligence, evolutionary, and heuristic optimization techniques to power system planning, operation, and control.

Dr. Abdelaziz is a member of IET and the Egyptian Sub-Committees of IEC and CIGRE'. He has been awarded many prizes for distinct researches and for international publishing from Ain Shams University and Future University in Egypt. He is the Chairman of the IEEE Education Society chapter in Egypt. He is a Senior Editor of *Ain Shams Engineering Journal*, an Editor of *Electric Power Components and Systems* journal, an Editorial Board member, an Editor, an Associate Editor, and an Editorial Advisory Board member for many international journals.

PAULO F. RIBEIRO (Fellow, IEEE) is currently a Full Professor with the Universidade Federal de Itajubá, Brazil, and a Fellow Researcher with the National Institute of Electric Energy (INERGE). He taught and worked in USA and The Netherlands, and was an Erskine Fellow with the University of Canterbury, New Zealand. He has written/edited four books and many book chapters and authored/coauthored over 375 articles. His research interests include power systems, power electronics, power quality, transmission and distribution systems, smart grids, energy storage systems, and philosophy of technology/systems engineering. He is a Fellow of the IET.

ZIAD M. ALI received the B.Sc. and M.Sc. degrees in electrical engineering from the Faculty of Engineering, Assiut University, Assuit, Egypt, in 1998 and 2003, respectively, and the Ph.D. degree from Kazan State Technical University, Tatarstan, Russia, in 2010. He worked as a Demonstrator at the Aswan Faculty of Engineering, South Valley University, Aswan, Egypt, and as an Assistant Lecturer at the Aswan Faculty of Engineering. He also worked as an Assistant Professor at the Aswan Faculty of Engineering, Egypt, from 2011 to 2016, as a Visitor Researcher at the Power System Laboratory, Kazan State Energy University, Russian, from 2012 to 2013, and as a Visitor Researcher at the Power System Laboratory, College of Engineering, University of Padova, Italy, from 2013 to 2014. He is currently working as an Associate Professor with the Electrical Department, College of Engineering at Wadi Addawasir, Prince Sattam Bin Abdulaziz University, Saudi Arabia. His research interests include power system analysis, FACTS, optimization, renewable energy analysis, smart grid, and material science.